

Tracking Tensor Ring Decompositions of Streaming Tensors

Yajie Yu · Hanyu Li

Received: date / Accepted: date

Abstract Tensor ring (TR) decomposition is an efficient approach to discover the hidden low-rank patterns for higher-order tensors, and streaming tensors are becoming highly prevalent in real-world applications. In this paper, we investigate how to track TR decompositions of streaming tensors. An efficient algorithm is first proposed. Then, based on this algorithm and randomized techniques, we present a randomized streaming TR decomposition. The proposed algorithms make full use of the structure of TR decomposition, and the randomized version can allow any sketching type. Theoretical results on sketch size are provided. In addition, the complexity analyses for the obtained algorithms are also given. We compare our proposals with the existing batch methods using both real and synthetic data. Numerical results show that they have better performance in computing time with maintaining similar accuracy.

Keywords Tensor ring decomposition · Streaming tensor · Randomized algorithm · Alternating least squares · Kronecker sub-sampled randomized Fourier transform · Uniform sampling · Importance sampling · Leverage scores

Mathematics Subject Classification (2000) 15A69 · 68W20

The work is supported by the National Natural Science Foundation of China (No. 11671060) and the Natural Science Foundation of Chongqing, China (No. cstc2019jcyj-msxmX0267)

Yajie Yu
College of Mathematics and Statistics, Chongqing University, Chongqing, 401331, P.R. China;
E-mail: zqyu@cqu.edu.cn

Hanyu Li
College of Mathematics and Statistics, Chongqing University, Chongqing, 401331, P.R. China;
E-mail: lihy.hy@gmail.com or hyli@cqu.edu.cn

1 Introduction

Tensor ring (TR) decomposition [34] is an important tool for higher-order data analysis. It decomposes an N th-order tensor into a cyclic interconnection of N 3rd-order tensors, and hence has the advantage of circular dimensional permutation invariance. Specifically, for a tensor $\mathcal{X} \in \mathbb{R}^{I_1 \times I_2 \times \cdots \times I_N}$, it has the TR format as follows

$$\mathcal{X}(i_1, \cdots, i_N) = \text{Trace}(\mathbf{G}_1(i_1)\mathbf{G}_2(i_2) \cdots \mathbf{G}_N(i_N)) = \text{Trace}\left(\prod_{n=1}^N \mathbf{G}_n(i_n)\right),$$

where $\mathbf{G}_n(i_n) = \mathcal{G}_n(:, i_n, :) \in \mathbb{R}^{R_n \times R_{n+1}}$ is the i_n -th *lateral slice* of the *core tensor (TR-core)* $\mathcal{G}_n \in \mathbb{R}^{R_n \times I_n \times R_{n+1}}$. Note that a *slice* is a 2nd-order section, i.e., a matrix, of a tensor obtained by fixing all the tensor indices but two. The sizes of TR-cores, i.e., R_k with $k = 1, \cdots, N$ and $R_{N+1} = R_1$, are called *TR-ranks*. Additionally, we use the notation $\text{TR}(\{\mathcal{G}_n\}_{n=1}^N)$ to denote the TR decomposition of a tensor.

In contrast to the two most popular tensor decompositions, i.e., CANDECOMP-PARAFAC (CP) and Tucker decompositions [13], TR decomposition avoids the NP-hard problem of computing the CP-rank and the curse of dimensionality due to the core tensor in Tucker decomposition. These advantages stem from the algorithms for finding TR-ranks being stable and the number of parameters of TR decomposition scaling linearly with the tensor order N . Furthermore, it is also feasible and convenient to directly implement some algebra operations in TR format [34], e.g., addition, dot product, norm, matrix-by-vector, etc., which is conducive to significantly enhancing the computational efficiency. Therefore, TR decomposition has already been utilized effectively in scientific computing to tackle intractable higher-dimensional and higher-order problems. This makes the problem of fitting $\text{TR}(\{\mathcal{G}_n\}_{n=1}^N)$ to a tensor \mathcal{X} be increasingly important.

The above fitting problem can be written as the following minimization problem:

$$\min_{\mathcal{G}_1, \cdots, \mathcal{G}_N} \|\text{TR}(\{\mathcal{G}_n\}_{n=1}^N) - \mathcal{X}\|_F, \quad (1.1)$$

where $\|\cdot\|_F$ denotes the Frobenius norm of a matrix or tensor. One standard computational method for this problem is to prescribe the fixed TR-ranks first, and then to determine the decomposition via alternating least squares (ALS). It is usually written as TR-ALS. Another classical method is to prescribe a fixed target accuracy first, and then to compute the decomposition via singular value decomposition. See [34, 19] for the details on these two methods. Moreover, with the rapid emergence of large-scale problems, the above two methods have been extended to randomized versions [32, 2, 18, 17, 30]. In addition, many other algorithms have also been proposed and developed for TR decomposition; see, e.g., [9, 1, 31]. However, all of these works are for the case that the whole tensor data \mathcal{X} is available and static.

As we know, in many practical applications, there only fragmentary data sets are initially available, with new data sets becoming available at the next

time step or appearing continuously over time. Live video broadcasts, surveillance videos, network flow, and social media data are examples. Such tensors are called streaming tensors or incremental/online tensors [22]. Developing streaming algorithms for TR decompositions, i.e., tracking TR decompositions, of such streaming tensors is both fascinating and necessary. This is because when the initial decomposition is already known, it is more expedient to update the streaming decomposition than to recalculate the entire decomposition. In previous research, some streaming methods have been successively presented for some other tensor decompositions; see e.g., [35, 16, 33] for CP decomposition, [21, 22, 5, 27, 23] for Tucker decomposition, and [15, 24, 14] for tensor train (TT) decomposition [20]. A more comprehensive and detailed overview can be found in [25]. However, streaming algorithms related to (instead of aiming at) TR decomposition have only been studied in several papers [10, 28, 11]. Specifically, He and Atia [10] developed a patch-tracking-based streaming TR completion framework for visual data recovery and devised a streaming algorithm that can update the latent TR-cores and complete the missing entries of patch tensors. Yu et al. [28] proposed an online TR subspace learning and imputation model by formulating exponentially weighted least squares with Frobenius norm regularization of TR-cores. The alternating recursive least squares and stochastic gradient algorithms were employed to solve the proposed model. Huang et al. [11] provided a multi-aspect streaming TR completion method. Whereas, all of these works didn't fully consider the special structure of TR decomposition. From [30, 29], it is shown that exploring the structure can significantly improve the efficiency of the related algorithms.

Therefore, in this paper, we focus on developing efficient ALS-based streaming algorithms for TR decomposition via making full use of its structure. Specifically, inspired by the work on CP decomposition in [35], we first propose an efficient streaming algorithm that can incrementally track TR decompositions of streaming tensors with any order. Then, motivated by the ideas in [16, 18, 30, 29], we derive a randomized streaming TR decomposition to deal with streaming large-scale tensors. Three randomized strategies, i.e., uniform sampling, leverage-based sampling, and Kronecker sub-sampled randomized Fourier transform (KSRFT), are used to reduce the dimension of the coefficient and unfolding matrices in the ALS subproblems, which makes the computing time and memory usage be reduced greatly. Moreover, these strategies can also avoid forming the full coefficient and sketching matrices and implementing matrix multiplication between large matrices.

The rest of this paper is organized as follows. Section 2 first gives some tensor notations and basic operations, and then briefly reviews the algorithms for TR decomposition. In Section 3, we present our streaming TR decomposition and its randomized variant as well as three sketching techniques. The evaluation of the computational performance of the proposed algorithms is reported in Section 4. Finally, Section 5 makes a conclusion and outlines some further directions. The missed proofs and the specific algorithms based on different sketches are given in Appendix A and Appendix B, respectively.

2 Preliminaries and Related Works

For convenience on the following presentment, we denote $[I] \stackrel{\text{def}}{=} \{1, \dots, I\}$ for a positive integer I , and set $\overline{i_1 i_2 \dots i_N} \stackrel{\text{def}}{=} 1 + \sum_{n=1}^N (i_n - 1) \prod_{j=1}^{n-1} I_j$ for the indices $i_1 \in [I_1], \dots, i_N \in [I_N]$.

Definition 2.1 Three unfolding matrices of a tensor $\mathcal{X} \in \mathbb{R}^{I_1 \times I_2 \times \dots \times I_N}$ are defined element-wise:

$$\begin{aligned} \text{Classical Mode-}n \text{ Unfolding: } & \mathbf{X}_{(n)}(i_n, \overline{i_1 \dots i_{n-1} i_{n+1} \dots i_N}) = \mathcal{X}(i_1, \dots, i_N), \\ \text{Mode-}n \text{ Unfolding: } & \mathbf{X}_{[n]}(i_n, \overline{i_{n+1} \dots i_N i_1 \dots i_{n-1}}) = \mathcal{X}(i_1, \dots, i_N), \\ n \text{ Unfolding: } & \mathbf{X}_{\langle n \rangle}(i_1, \dots, i_n, \overline{i_{n+1} \dots i_N}) = \mathcal{X}(i_1, \dots, i_N), \end{aligned}$$

which are of size $I_n \times \prod_{j \neq n} I_j$, $I_n \times \prod_{j \neq n} I_j$, and $\prod_{j=1}^n I_j \times \prod_{j=n+1}^N I_j$, respectively.

Definition 2.2 (TTM) The **tensor-times-matrix (TTM) multiplication** of a tensor $\mathcal{X} \in \mathbb{R}^{I_1 \times I_2 \times \dots \times I_N}$ and a matrix $\mathbf{U} \in \mathbb{R}^{J \times I_n}$ is a tensor of size $I_1 \times \dots \times I_{n-1} \times J \times I_{n+1} \times \dots \times I_N$ denoted by $\mathcal{X} \times_n \mathbf{U}$ and defined element-wise via

$$(\mathcal{X} \times_n \mathbf{U})(i_1, \dots, i_{n-1}, j, i_{n+1}, \dots, i_N) = \sum_{i_n=1}^{I_n} \mathcal{X}(i_1, \dots, i_n, \dots, i_N) \mathbf{U}(j, i_n).$$

Multiplying an N th-order tensor by multiple matrices on distinct modes is known as *Multi-TTM*. In particular, multiplying an N th-order tensor by the matrices \mathbf{U}_j with $j = 1, \dots, N$ in each mode implies $\mathcal{Y} = \mathcal{X} \times_1 \mathbf{U}_1 \times_2 \mathbf{U}_2 \dots \times_N \mathbf{U}_N$. Its mode- n unfolding can be presented as follows:

$$\mathbf{Y}_{[n]} = \mathbf{U}_n \mathbf{X}_{[n]} (\mathbf{U}_{n-1} \otimes \dots \otimes \mathbf{U}_1 \otimes \mathbf{U}_N \otimes \dots \otimes \mathbf{U}_{n+1})^\top. \quad (2.1)$$

We now detail the TR-ALS mentioned in Section 1, which is a popular algorithm for TR decomposition. To achieve this, we need the following definition.

Definition 2.3 Let $\mathcal{X} = \text{TR}(\{\mathcal{G}_n\}_{n=1}^N) \in \mathbb{R}^{I_1 \times I_2 \times \dots \times I_N}$. The **subchain tensor** $\mathcal{G}^{\neq n} \in \mathbb{R}^{R_{n+1} \times \prod_{j \neq n} I_j \times R_n}$ is the merging of all TR-cores except the n -th one and can be written slice-wise via

$$\mathcal{G}^{\neq n}(\overline{i_{n+1} \dots i_N i_1 \dots i_{n-1}}) = \prod_{j=n+1}^N \mathbf{G}_j(i_j) \prod_{j=1}^{n-1} \mathbf{G}_j(i_j).$$

Thus, according to Theorem 3.5 in [34], the objective in (1.1) can be rewritten as the following N subproblems

$$\mathbf{G}_{n(2)} = \arg \min_{\mathbf{G}_{n(2)}} \frac{1}{2} \left\| \mathcal{G}^{\neq n} \mathbf{G}_{n(2)}^\top - \mathbf{X}_{[n]}^\top \right\|_F, \quad n = 1, \dots, N. \quad (2.2)$$

Algorithm 1 TR-ALS [34]

Input: $\mathcal{X} \in \mathbb{R}^{I_1 \times \dots \times I_N}$, TR-ranks R_1, \dots, R_N
Output: TR-cores $\{\mathcal{G}_n \in \mathbb{R}^{R_n \times I_n \times R_{n+1}}\}_{n=1}^N$

- 1: Initialize TR-cores $\mathcal{G}_1, \dots, \mathcal{G}_N$
- 2: **repeat**
- 3: **for** $n = 1, \dots, N$ **do**
- 4: Compute $\mathbf{G}_{[2]}^{\neq n}$ from TR-cores
- 5: Update $\mathcal{G}_n = \arg \min_{\mathcal{G}_n} \left\| \mathbf{G}_{[2]}^{\neq n} \mathbf{G}_n^\top - \mathbf{X}_{[n]}^\top \right\|_F$
- 6: **end for**
- 7: **until** termination criteria met

The so-called TR-ALS is a method that keeps all TR-cores fixed except the n -th one and finds the solution to the LS problem (2.2) with respect to it. We summarize the method in Algorithm 1.

However, TR-ALS does not fully utilize the structure of the coefficient matrix $\mathbf{G}_{[2]}^{\neq n}$. Yu and Li [29] fixed this issue recently and proposed a more efficient algorithm called TR-ALS-NE, which is the basis of our first algorithm in the present paper. We first list the required definitions and property before detailing the algorithm in Algorithm 2.

Definition 2.4 (Outer Product) The **outer product** of two tensors $\mathcal{A} \in \mathbb{R}^{I_1 \times \dots \times I_N}$ and $\mathcal{B} \in \mathbb{R}^{J_1 \times \dots \times J_M}$ is a tensor of size $I_1 \times \dots \times I_N \times J_1 \times \dots \times J_M$ denoted by $\mathcal{A} \circ \mathcal{B}$ and defined element-wise via

$$(\mathcal{A} \circ \mathcal{B})(i_1, \dots, i_N, j_1, \dots, j_M) = \mathcal{A}(i_1, \dots, i_N) \mathcal{B}(j_1, \dots, j_M).$$

Definition 2.5 (General Contracted Tensor Product) The **general contracted tensor product** of two tensors $\mathcal{A} \in \mathbb{R}^{I_1 \times J \times R_1 \times K}$ and $\mathcal{B} \in \mathbb{R}^{J \times I_2 \times K \times R_2}$ is a tensor of size $I_1 \times I_2 \times R_1 \times R_2$ denoted by $\mathcal{A} \times_{2,4}^{1,3} \mathcal{B}$ and defined element-wise via

$$(\mathcal{A} \times_{2,4}^{1,3} \mathcal{B})(i_1, i_2, r_1, r_2) = \sum_{j,k} \mathcal{A}(i_1, j, r_1, k) \mathcal{B}(j, i_2, k, r_2).$$

Definition 2.6 (Subchain Product [30]) The **mode-2 subchain product** of two tensors $\mathcal{A} \in \mathbb{R}^{I_1 \times J_1 \times K}$ and $\mathcal{B} \in \mathbb{R}^{K \times J_2 \times I_2}$ is a tensor of size $I_1 \times J_1 J_2 \times I_2$ denoted by $\mathcal{A} \boxtimes_2 \mathcal{B}$ and defined as

$$(\mathcal{A} \boxtimes_2 \mathcal{B})(\overline{j_1 j_2}) = \mathbf{A}(j_1) \mathbf{B}(j_2).$$

Proposition 2.1 [29] Let $\mathcal{A} \in \mathbb{R}^{I_1 \times J \times K_1}$, $\mathcal{B} \in \mathbb{R}^{K_1 \times R \times L_1}$, $\mathcal{C} \in \mathbb{R}^{I_2 \times J \times K_2}$ and $\mathcal{D} \in \mathbb{R}^{K_2 \times R \times L_2}$ be 3rd-order tensors. Then

$$(\mathcal{A} \boxtimes_2 \mathcal{B})_{[2]}^\top (\mathcal{C} \boxtimes_2 \mathcal{D})_{[2]} = \left(\left(\sum_{r=1}^R \mathbf{B}(r)^\top \circ \mathbf{D}(r)^\top \right) \times_{2,4}^{1,3} \left(\sum_{j=1}^J \mathbf{A}(j)^\top \circ \mathbf{C}(j)^\top \right) \right)_{\langle 2 \rangle}.$$

Algorithm 2 TR-ALS-NE [29]

Input: $\mathcal{X} \in \mathbb{R}^{I_1 \times \dots \times I_N}$, TR-ranks R_1, \dots, R_N
Output: TR-cores $\{\mathcal{G}_n \in \mathbb{R}^{R_n \times I_n \times R_{n+1}}\}_{n=1}^N$

- 1: Initialize TR-cores $\mathcal{G}_1, \dots, \mathcal{G}_N$
- 2: Compute $\mathcal{Z}_1 = \sum_{i_1=1}^{I_1} \mathbf{G}_1(i_1)^\top \circ \mathbf{G}_1(i_1)^\top, \dots, \mathcal{Z}_N = \sum_{i_N=1}^{I_N} \mathbf{G}_N(i_N)^\top \circ \mathbf{G}_N(i_N)^\top$
- 3: **repeat**
- 4: **for** $n = 1, \dots, N$ **do**
- 5: $\mathcal{H}^{\neq n} \leftarrow \mathcal{Z}_{n-1} \times_{2,4}^{1,3} \dots \times_{2,4}^{1,3} \mathcal{Z}_1 \times_{2,4}^{1,3} \mathcal{Z}_N \times_{2,4}^{1,3} \dots \times_{2,4}^{1,3} \mathcal{Z}_{n+1}$
- 6: $\mathcal{G}^{\neq n} \leftarrow \mathcal{G}_{n+1} \boxtimes_2 \dots \boxtimes_2 \mathcal{G}_N \boxtimes_2 \mathcal{G}_1 \boxtimes_2 \dots \boxtimes_2 \mathcal{G}_{n-1} \triangleright$ From Definitions 2.3 and 2.6
- 7: $\mathbf{M}_n \leftarrow \mathbf{X}_{[n]} \mathbf{G}_{[2]}^{\neq n}$
- 8: Solve $\mathbf{G}_{n(2)} \mathbf{H}_{\langle 2 \rangle}^{\neq n} = \mathbf{M}_n$
- 9: Recompute $\mathcal{Z}_n = \sum_{i_n=1}^{I_n} \mathbf{G}_n(i_n)^\top \circ \mathbf{G}_n(i_n)^\top$ for the updated TR-core \mathcal{G}_n
- 10: **end for**
- 11: **until** termination criteria met

As mentioned in Section 1, randomized methods have been proposed for TR-ALS [18, 17, 30]. Among them, the most relevant algorithms to this paper are TR-ALS-Sampled [18] and TR-KSRFT-ALS [30]. The sampling techniques of these two algorithms will be detailed in Algorithm 3 after introducing an additional definition.

Definition 2.7 (Slices-Hadamard product [30]) The **mode-2 slices-Hadamard product** of two tensors \mathcal{A} and \mathcal{B} is a tensor of size $I_1 \times J \times I_2$ denoted by $\mathcal{A} \boxtimes_2 \mathcal{B}$ and defined as

$$(\mathcal{A} \boxtimes_2 \mathcal{B})(j) = \mathbf{A}(j)\mathbf{B}(j).$$

Algorithm 3 Sampled subchain and input tensors (SSIT), summarized from [18] and [30]

Input: TR-cores $\{\mathcal{G}_k \in \mathbb{R}^{R_k \times I_k \times R_{k+1}}\}_{k=1, k \neq n}^N$, sampling size m , probability distributions $\{\mathbf{p}_k\}_{k=1, k \neq n}^N$

Output: sampled subchain tensor $\mathcal{G}_S^{\neq n}$, sampled input tensor $\mathbf{X}_{S[n]}$

- 1: $\text{idxs} \leftarrow \text{ZEROS}(m, N-1)$
- 2: **for** $k = n+1, \dots, N, 1, \dots, n-1$ **do**
- 3: $\text{idxs}(:, k) \leftarrow \text{RANDSAMPLE}(I_k, m, \text{true}, \mathbf{p}_k)$
- 4: **end for**
- 5: Let $\mathcal{G}_S^{\neq n}$ be a tensor of size $R_{n+1} \times m \times R_{n+1}$, where every lateral slice is an $R_{n+1} \times R_{n+1}$ identity matrix
- 6: **for** $k = n+1, \dots, N, 1, \dots, n-1$ **do**
- 7: $\mathcal{G}_S^{\neq n} \leftarrow \mathcal{G}_S^{\neq n} \boxtimes_2 \mathcal{G}_k(:, \text{idxs}(:, k), :)$
- 8: **end for**
- 9: $\mathbf{X}_{S[n]} \leftarrow \text{MODE-N-UNFOLDING}(\mathcal{X}(\text{idxs}(:, 1), \dots, \text{idxs}(:, n-1), :, \text{idxs}(:, n+1), \dots, \text{idxs}(:, N))))$

3 Proposed Methods

We first propose a streaming algorithm for tracking TR decomposition, and then present its randomized variant. After that, three different sketching techniques based on uniform sampling, leverage-based sampling, and KSRFT, are discussed.

3.1 Streaming TR Decomposition

Let $\mathbf{X}^{old} \in \mathbb{R}^{I_1 \times \dots \times I_{N-1} \times t^{old}}$ with the N -th mode being the time, and its TR decomposition be $\text{TR}(\{\mathbf{G}_n^{old}\}_{n=1}^N)$. Now assume that, at the *time step* τ , a *temporal slice* $\mathbf{X}^{new} \in \mathbb{R}^{I_1 \times \dots \times I_{N-1} \times t^{new}}$ is added to \mathbf{X}^{old} to form a tensor $\mathbf{X} \in \mathbb{R}^{I_1 \times \dots \times I_{N-1} \times (t^{old} + t^{new})}$, where $t^{old} \gg t^{new}$. We are interested in finding the TR decomposition $\text{TR}(\{\mathbf{G}_n\}_{n=1}^N)$ of \mathbf{X} with the help of $\text{TR}(\{\mathbf{G}_n^{old}\}_{n=1}^N)$ and the existing intermediate information. In the following, we give the detailed updating formulations.

Update Temporal Mode We first consider the update for the TR-core of the temporal mode, i.e., \mathbf{G}_N , by fixing the other TR-cores. Specifically, by (2.2), we have

$$\begin{aligned} \mathbf{G}_{N(2)} &\leftarrow \arg \min_{\mathbf{G}_{N(2)}} \frac{1}{2} \left\| \mathbf{X}_{[N]} - \mathbf{G}_{N(2)} (\mathbf{G}_{[2]}^{\neq N})^\top \right\|_F \\ &= \arg \min_{\mathbf{G}_{N(2)}} \frac{1}{2} \left\| \begin{bmatrix} \mathbf{X}_{[N]}^{old} \\ \mathbf{X}_{[N]}^{new} \end{bmatrix} - \begin{bmatrix} \mathbf{G}_{N(2)}^{(1)} \\ \mathbf{G}_{N(2)}^{(2)} \end{bmatrix} (\mathbf{G}_{[2]}^{\neq N})^\top \right\|_F. \end{aligned}$$

With Proposition 2.1 and the fact from [30],

$$\mathbf{G}^{\neq n} = \mathbf{G}_{n+1} \boxtimes_2 \dots \boxtimes_2 \mathbf{G}_N \boxtimes_2 \mathbf{G}_1 \boxtimes_2 \dots \boxtimes_2 \mathbf{G}_{n-1}, \quad (3.1)$$

it is clear that

$$\mathbf{G}_{N(2)} \leftarrow \begin{bmatrix} \mathbf{X}_{[N]}^{old} \mathbf{G}_{[2]}^{\neq N} \left((\mathbf{G}_{[2]}^{\neq N})^\top \mathbf{G}_{[2]}^{\neq N} \right)^\dagger \\ \mathbf{X}_{[N]}^{new} \mathbf{G}_{[2]}^{\neq N} \left((\mathbf{G}_{[2]}^{\neq N})^\top \mathbf{G}_{[2]}^{\neq N} \right)^\dagger \end{bmatrix} = \begin{bmatrix} \mathbf{G}_{N(2)}^{old} \\ \mathbf{X}_{[N]}^{new} \mathbf{G}_{[2]}^{\neq N} \left(\mathbf{H}_{\langle 2 \rangle}^{\neq N} \right)^\dagger \end{bmatrix} = \begin{bmatrix} \mathbf{G}_{N(2)}^{old} \\ \mathbf{G}_{N(2)}^{new} \end{bmatrix},$$

where $\mathbf{H}_{\langle 2 \rangle}^{\neq N} = \mathbf{Z}_{N-1} \times_{2,4}^{1,3} \dots \times_{2,4}^{1,3} \mathbf{Z}_1$ with $\mathbf{Z}_j = \sum_{i_j=1}^{I_j} \mathbf{G}_j(i_j)^\top \circ \mathbf{G}_j(i_j)^\top$. Thus,

$$\mathbf{G}_{N(2)}^{new} \leftarrow \mathbf{X}_{[N]}^{new} \mathbf{G}_{[2]}^{\neq N} \left(\mathbf{H}_{\langle 2 \rangle}^{\neq N} \right)^\dagger, \quad \mathbf{G}_{N(2)} \leftarrow \begin{bmatrix} \mathbf{G}_{N(2)}^{old} \\ \mathbf{G}_{N(2)}^{new} \end{bmatrix}.$$

Update Non-temporal Modes For each non-temporal mode $n \in [N - 1]$, we now consider the update of \mathcal{G}_n by fixing the remain TR-cores. Specifically, according to (2.2), we have the following normal equation

$$\begin{aligned}
0 &= \mathbf{X}_{[n]} \underbrace{\begin{pmatrix} \boxtimes_2 & \mathcal{G}_j \\ n+1, \dots, N, \\ 1, \dots, n-1 \end{pmatrix}}_{\mathbf{P}_n} \underset{[2]}{=} - \mathbf{G}_{n(2)} \underbrace{\begin{pmatrix} \boxtimes_2 & \mathcal{G}_j \\ n+1, \dots, N, \\ 1, \dots, n-1 \end{pmatrix}^\top}_{\mathbf{Q}_n} \underset{[2]}{\begin{pmatrix} \boxtimes_2 & \mathcal{G}_j \\ n+1, \dots, N, \\ 1, \dots, n-1 \end{pmatrix}} \\
&= \begin{bmatrix} \mathbf{X}_{[n]}^{old} & \mathbf{X}_{[n]}^{new} \end{bmatrix} \begin{bmatrix} (\mathbf{G}_{old}^{\neq n})_{[2]} \\ (\mathbf{G}_{new}^{\neq n})_{[2]} \end{bmatrix} - \mathbf{G}_{n(2)} \begin{bmatrix} (\mathbf{G}_{old}^{\neq n})_{[2]}^\top & (\mathbf{G}_{new}^{\neq n})_{[2]}^\top \end{bmatrix} \begin{bmatrix} (\mathbf{G}_{old}^{\neq n})_{[2]} \\ (\mathbf{G}_{new}^{\neq n})_{[2]} \end{bmatrix} \\
&= \left(\mathbf{P}_n^{old} + \mathbf{X}_{[n]}^{new} (\mathbf{G}_{new}^{\neq n})_{[2]} \right) - \mathbf{G}_{n(2)} \left(\mathbf{Q}_n^{old} + (\mathbf{H}_{new}^{\neq n})_{\langle 2 \rangle} \right), \quad (3.2)
\end{aligned}$$

where

$$\mathcal{G}_{old}^{\neq n} = \begin{pmatrix} \boxtimes_2 & \mathcal{G}_j \\ n+1, \dots, N-1 \end{pmatrix} \boxtimes_2 \mathcal{G}_N^{old} \boxtimes_2 \begin{pmatrix} \boxtimes_2 & \mathcal{G}_j \\ 1, \dots, n-1 \end{pmatrix}, \quad (3.3)$$

$$\mathcal{G}_{new}^{\neq n} = \begin{pmatrix} \boxtimes_2 & \mathcal{G}_j \\ n+1, \dots, N-1 \end{pmatrix} \boxtimes_2 \mathcal{G}_N^{new} \boxtimes_2 \begin{pmatrix} \boxtimes_2 & \mathcal{G}_j \\ 1, \dots, n-1 \end{pmatrix}, \quad (3.4)$$

$$\mathcal{H}_{new}^{\neq n} = \begin{pmatrix} \times_{2,4}^{1,3} & \mathcal{Z}_j \\ n-1, \dots, 1 \end{pmatrix} \times_{2,4}^{1,3} \mathcal{Z}_N^{new} \times_{2,4}^{1,3} \begin{pmatrix} \times_{2,4}^{1,3} & \mathcal{Z}_j \\ N-1, \dots, n+1 \end{pmatrix}$$

with

$$\mathcal{Z}_N^{new} = \sum_{i_N=1}^{I_N} \mathbf{G}_N^{new}(i_N)^\top \circ \mathbf{G}_N^{new}(i_N)^\top.$$

Note that to derive (3.2), Proposition 2.1, (3.1), and the permutation matrix $\mathbf{\Pi}_n$ defined as

$$(\mathbf{X}_{[n]} \mathbf{\Pi}_n) (\overline{:, i_1 \dots i_{n-1} i_{n+1} \dots i_N}) = \mathbf{X}_{[n]} (\overline{:, i_{n+1} \dots i_N i_1 \dots i_{n-1}})$$

such that

$$\begin{aligned}
\mathbf{X}_{[n]} \mathbf{\Pi}_n \mathbf{\Pi}_n^\top \begin{pmatrix} \boxtimes_2 & \mathcal{G}_j \\ n+1, \dots, N, \\ 1, \dots, n-1 \end{pmatrix} \underset{[2]}{=} &= \begin{bmatrix} \mathbf{X}_{[n]}^{old} & \mathbf{X}_{[n]}^{new} \end{bmatrix} \begin{bmatrix} (\mathbf{G}_{old}^{\neq n})_{[2]} \\ (\mathbf{G}_{new}^{\neq n})_{[2]} \end{bmatrix} \\
\begin{pmatrix} \boxtimes_2 & \mathcal{G}_j \\ n+1, \dots, N, \\ 1, \dots, n-1 \end{pmatrix} \underset{[2]}{=} & \mathbf{\Pi}_n \mathbf{\Pi}_n^\top \begin{pmatrix} \boxtimes_2 & \mathcal{G}_j \\ n+1, \dots, N, \\ 1, \dots, n-1 \end{pmatrix} \underset{[2]}{=} \begin{bmatrix} (\mathbf{G}_{old}^{\neq n})_{[2]}^\top & (\mathbf{G}_{new}^{\neq n})_{[2]}^\top \end{bmatrix} \begin{bmatrix} (\mathbf{G}_{old}^{\neq n})_{[2]} \\ (\mathbf{G}_{new}^{\neq n})_{[2]} \end{bmatrix}
\end{aligned}$$

have been used. Thus, we achieve the update for \mathcal{G}_n as follows

$$\begin{aligned}
\mathbf{P}_n &\leftarrow \mathbf{P}_n^{old} + \mathbf{X}_{[n]}^{new} (\mathbf{G}_{new}^{\neq n})_{[2]}, \quad \mathbf{Q}_n \leftarrow \mathbf{Q}_n^{old} + (\mathbf{H}_{new}^{\neq n})_{\langle 2 \rangle}, \\
\mathbf{G}_{n(2)} &\leftarrow \mathbf{P}_n \mathbf{Q}_n^\dagger.
\end{aligned}$$

The whole process for streaming TR decomposition is summarized in Algorithm 4, from which we find that the information of previous decomposition can be stored in the complementary matrices \mathbf{P}_n and \mathbf{Q}_n , and hence the expensive computation can be avoided and the TR-cores can be efficiently updated in an incremental way.

Algorithm 4 Streaming TR decomposition (STR)

Input: Initial tensor \mathcal{X}^{init} , TR-ranks R_1, \dots, R_N and new data tensor \mathcal{X}^{new}
Output: TR-cores $\{\mathcal{G}_n \in \mathbb{R}^{R_n \times I_n \times R_{n+1}}\}_{n=1}^N$

// Initialization stage
 1: Compute initial TR-cores $\mathcal{G}_1, \dots, \mathcal{G}_N$ of \mathcal{X}^{init}
 2: Compute the Gram tensors $\mathcal{Z}_1 = \sum_{i_1=1}^{I_1} \mathbf{G}_1(i_1)^\top \circ \mathbf{G}_1(i_1)^\top, \dots, \mathcal{Z}_{N-1} = \sum_{i_{N-1}=1}^{I_{N-1}} \mathbf{G}_{N-1}(i_{N-1})^\top \circ \mathbf{G}_{N-1}(i_{N-1})^\top$
 3: **for** $n = 1, \dots, N - 1$ **do**
 4: $\mathbf{P}_n \leftarrow \mathbf{X}_{[n]}^{init} \mathbf{G}_{[2]}^{\neq n}$
 5: $\mathbf{Q}_n \leftarrow \left(\begin{array}{c} \times_{2,4}^{1,3} \mathcal{Z}_j \\ n-1, \dots, 1 \\ N, \dots, n+1 \end{array} \right)_{\langle 2 \rangle}$
 6: **end for**
 7: **for** $\tau = 1, \dots, t$ time steps **do**
 // Update stage for temporal mode
 8: $\mathcal{H}^{\neq N} \leftarrow \mathcal{Z}_{N-1} \times_{2,4}^{1,3} \dots \times_{2,4}^{1,3} \mathcal{Z}_1$
 9: $\mathbf{G}_{N(2)}^{new} \leftarrow \mathbf{X}_{[N]}^{new} \mathbf{G}_{[2]}^{\neq N} (\mathcal{H}^{\neq N})^\dagger$
 10: $\mathbf{G}_{N(2)} \leftarrow \begin{bmatrix} \mathbf{G}_{N(2)}^{old} \\ \mathbf{G}_{N(2)}^{new} \end{bmatrix}$ and reshape $\mathbf{G}_{N(2)}$ to \mathcal{G}_N
 11: $\mathcal{Z}_N \leftarrow \sum_{i_N=1}^{I_N} \mathbf{G}_N(i_N)^\top \circ \mathbf{G}_N(i_N)^\top$
 // Update stage for non-temporal modes
 12: **for** $n = 1, \dots, N - 1$ **do**
 13: $\mathcal{G}_{new}^{\neq n} \leftarrow \left(\begin{array}{c} \boxtimes_2 \mathcal{G}_j \\ n+1, \dots, N-1 \end{array} \right) \boxtimes_2 \mathcal{G}_N^{new} \boxtimes_2 \left(\begin{array}{c} \boxtimes_2 \mathcal{G}_j \\ 1, \dots, n-1 \end{array} \right)$
 14: $\mathbf{P}_n \leftarrow \mathbf{P}_n + \mathbf{X}_{[n]}^{new} (\mathcal{G}_{new}^{\neq n})_{[2]}$
 15: $\mathcal{H}_{new}^{\neq n} = \left(\begin{array}{c} \times_{2,4}^{1,3} \mathcal{Z}_j \\ n-1, \dots, 1 \end{array} \right) \times_{2,4}^{1,3} \mathcal{Z}_N^{new} \times_{2,4}^{1,3} \left(\begin{array}{c} \times_{2,4}^{1,3} \mathcal{Z}_j \\ N-1, \dots, n+1 \end{array} \right)$
 16: $\mathbf{Q}_n \leftarrow \mathbf{Q}_n + (\mathcal{H}_{new}^{\neq n})_{\langle 2 \rangle}$
 17: $\mathbf{G}_{n(2)} \leftarrow \mathbf{P}_n \mathbf{Q}_n^\dagger$ and reshape $\mathbf{G}_{n(2)}$ to \mathcal{G}_n
 18: $\mathcal{Z}_n \leftarrow \sum_{i_n=1}^{I_n} \mathbf{G}_n(i_n)^\top \circ \mathbf{G}_n(i_n)^\top$
 19: **end for**
 20: **end for**

Remark 3.1 With regard to the initialization of streaming TR decomposition, i.e., Line 1 in Algorithm 4, we can choose any feasible techniques. Inspired by the experimental results in [16, Section III.B], we recommend running the corresponding offline version of Algorithm 4 for finding the initial values. However, in the specific numerical experiments later in this paper, we use the same

initial values for various algorithms for convenience; see the detailed description of experiments in Section 4. The above explanation is also applicable to Algorithm 5 below.

Remark 3.2 From the derivation of Algorithm 4, it can be seen that the structure of the coefficient matrices in the subproblems is well used. That is, Proposition 2.1 is employed to reduce the computational cost. Hence, the algorithm is more efficient than applying TR-ALS directly. More descriptions and comparisons on advantages for using Proposition 2.1 can be found in [29].

Remark 3.3 As we know, TR decomposition generalizes the famous TT decomposition by relaxing some constraints [34]. So, with a slight change, Algorithm 4 is also applicable to TT decomposition. It is worthy to emphasize that the corresponding method is very different from the ones in [15, 24, 14] mentioned in Section 1. The main difference still lies in that we make full use of the structure introduced before.

3.2 Randomized Streaming TR Decomposition

We now employ randomized sketching techniques to improve the efficiency of streaming TR decomposition. That is, we consider the following sketched subproblems for streaming tensor with the sketching matrices $\Psi_n \in \mathbb{R}^{m \times \prod_{j \neq N} I_j}$,

$$\arg \min_{\mathbf{G}_{n(2)}} \left\| \Psi_n \mathbf{G}_{[2]}^{\neq n} \mathbf{G}_{n(2)}^\top - \Psi_n \mathbf{X}_{[n]}^\top \right\|_F, \quad n = 1, \dots, N. \quad (3.5)$$

A randomized streaming TR decomposition will be proposed. In the following, we give the specific updating rules.

Update Temporal Mode By dividing the corresponding terms into two parts, from (3.5), we have

$$\mathbf{G}_{N(2)} \leftarrow \arg \min_{\mathbf{G}_{N(2)}} \frac{1}{2} \left\| \begin{bmatrix} \mathbf{X}_{[N]}^{\text{old}} (\Psi_N^{\text{old}})^\top \\ \mathbf{X}_{[N]}^{\text{new}} (\Psi_N^{\text{new}})^\top \end{bmatrix} - \begin{bmatrix} \mathbf{G}_{N(2)}^{(1)} (\Psi_N^{\text{old}} \mathbf{G}_{[2]}^{\neq N})^\top \\ \mathbf{G}_{N(2)}^{(2)} (\Psi_N^{\text{new}} \mathbf{G}_{[2]}^{\neq N})^\top \end{bmatrix} \right\|_F,$$

where $\Psi_N^{\text{old}} \in \mathbb{R}^{m \times \prod_{j \neq N} I_j}$ and $\Psi_N^{\text{new}} \in \mathbb{R}^{m \times \prod_{j \neq N} I_j}$. It is clear that

$$\begin{aligned} \mathbf{G}_{N(2)} &\leftarrow \begin{bmatrix} \mathbf{X}_{[N]}^{\text{old}} (\Psi_N^{\text{old}})^\top \left((\Psi_N^{\text{old}} \mathbf{G}_{[2]}^{\neq N})^\top \right)^\dagger \\ \mathbf{X}_{[N]}^{\text{new}} (\Psi_N^{\text{new}})^\top \left((\Psi_N^{\text{new}} \mathbf{G}_{[2]}^{\neq N})^\top \right)^\dagger \end{bmatrix} \\ &= \begin{bmatrix} \mathbf{G}_{N(2)}^{\text{old}} \\ \mathbf{X}_{[N]}^{\text{new}} (\Psi_N^{\text{new}})^\top \left((\Psi_N^{\text{new}} \mathbf{G}_{[2]}^{\neq N})^\top \right)^\dagger \end{bmatrix} = \begin{bmatrix} \mathbf{G}_{N(2)}^{\text{old}} \\ \mathbf{G}_{N(2)}^{\text{new}} \end{bmatrix}. \end{aligned}$$

Thus,

$$\mathbf{G}_{N(2)}^{\text{new}} \leftarrow \mathbf{X}_{[N]}^{\text{new}} (\Psi_N^{\text{new}})^\top \left((\Psi_N^{\text{new}} \mathbf{G}_{[2]}^{\neq N})^\top \right)^\dagger, \quad \mathbf{G}_{N(2)} \leftarrow \begin{bmatrix} \mathbf{G}_{N(2)}^{\text{old}} \\ \mathbf{G}_{N(2)}^{\text{new}} \end{bmatrix}.$$

Remark 3.4 Usually, the sketching matrix Ψ_N^{new} is not the same as Ψ_N^{old} , which implies that $\mathbf{X}_{[N]}^{new}$ will be sketched at each time step.

Update Non-temporal Modes As done for streaming TR decomposition in Section 3.1 and similar to the above deduction, we have

$$\begin{aligned}\mathbf{P}_n &\leftarrow \mathbf{P}_n^{old} + \mathbf{X}_{[n]}^{new} (\Psi_n^{new})^\top \Psi_n^{new} (\mathbf{G}_{new}^{\neq n})_{[2]}, \\ \mathbf{Q}_n &\leftarrow \mathbf{Q}_n^{old} + (\mathbf{G}_{new}^{\neq n})_{[2]}^\top (\Psi_n^{new})^\top \Psi_n^{new} (\mathbf{G}_{new}^{\neq n})_{[2]}, \\ \mathbf{G}_{n(2)} &\leftarrow \mathbf{P}_n \mathbf{Q}_n^\dagger,\end{aligned}$$

where $\Psi_n^{old} \in \mathbb{R}^{m \times \prod_{j \neq n} I_j}$ and $\Psi_n^{new} \in \mathbb{R}^{m \times \prod_{j \neq n} I_j}$ are sketching matrices and the other notations are the same as the ones in (3.2), (3.3), and (3.4).

Remark 3.5 Unlike the case for streaming TR decomposition in Section 3.1, here the calculation of the Gram matrix $(\mathbf{G}_{new}^{\neq n})_{[2]}^\top (\Psi_n^{new})^\top \Psi_n^{new} (\mathbf{G}_{new}^{\neq n})_{[2]}$ is quite cheap. So, we do not consider its structure any more though it still exists. Instead, we mainly focus on how to compute $\Psi_n^{new} (\mathbf{G}_{new}^{\neq n})_{[2]}$ fast by using the structure of $(\mathbf{G}_{new}^{\neq n})_{[2]}$ and choosing suitable Ψ_n^{new} ; see Section 3.3 below.

The whole process for randomized streaming TR decomposition is summarized in Algorithm 5, which shows that, as carried out by Algorithm 3 or Algorithm 6, different sketching techniques can be used to compute the sketched subchain and input tensors. Moreover, when forming the aforementioned sketched tensors, the un-updated TR-cores and fibers do not need to be sketched again. The corresponding detailed algorithms are presented in Appendix B. Note that, in this case, the theoretical guarantees given in Section 3.3 still apply.

3.3 Different Sketching Techniques

We mainly consider three practical sketching techniques: Uniform sampling, leverage-based sampling, and KSRFT.

Uniform Sampling That is,

$$\Psi_n = \mathbf{D}_n \mathbf{S}_n, \quad (3.6)$$

where $\mathbf{S}_n \in \mathbb{R}^{m \times J_n}$ with

$$J_n = \begin{cases} I_1 I_2 \cdots I_{N-1}, & n = N \\ I_1 I_2 \cdots I_{n-1} I_{n+1} \cdots I_{N-1} t^{new}, & n \neq N \end{cases}$$

is a sampling matrix, i.e.,

$$(\mathbf{S}_n)_{ij} = \begin{cases} 1, & \text{if the } j\text{-th row is chosen in the } i\text{-th independent random trial} \\ & \text{with the probability } 1/J_n, \\ 0, & \text{otherwise,} \end{cases}$$

Algorithm 5 Randomized streaming TR decomposition (rSTR)

Input: Initial tensor \mathcal{X}^{init} , TR-ranks R_1, \dots, R_N , new data tensor \mathcal{X}^{new} and sketch size m

Output: TR-cores $\{\mathcal{G}_n \in \mathbb{R}^{R_n \times I_n \times R_{n+1}}\}_{n=1}^N$

```

// Initialization stage
1: Compute initial TR-cores  $\mathcal{G}_1, \dots, \mathcal{G}_N$  of  $\mathcal{X}^{init}$ 
2: for  $n = 1, \dots, N - 1$  do
3:   Compute  $\mathcal{G}_S^{\neq n}$  and  $\mathbf{X}_{S[n]}^{init}$  using Algorithm 3 or Algorithm 6
4:    $\mathbf{P}_n \leftarrow \mathbf{X}_{S[n]}^{init} \mathbf{G}_{S[2]}^{\neq n}$ 
5:    $\mathbf{Q}_n \leftarrow (\mathbf{G}_{S[2]}^{\neq n})^\top \mathbf{G}_{S[2]}^{\neq n}$ 
6: end for
7: for  $\tau = 1, \dots, t$  time steps do
  // Update stage for temporal mode
8:   Compute  $\mathcal{G}_S^{\neq N}$  and  $\mathbf{X}_{S[N]}^{new}$  using Algorithm 3 or Algorithm 6
9:    $\mathbf{G}_{N(2)}^{new} \leftarrow \mathbf{X}_{S[N]}^{new} \left( (\mathbf{G}_{S[2]}^{\neq N})^\top \right)^\dagger$ 
10:   $\mathbf{G}_{N(2)} \leftarrow \begin{bmatrix} \mathbf{G}_{N(2)}^{old} \\ \mathbf{G}_{N(2)}^{new} \end{bmatrix}$  and reshape  $\mathbf{G}_{N(2)}$  to  $\mathcal{G}_N$ 
  // Update stage for non-temporal modes
11:  for  $n = 1, \dots, N - 1$  do
12:     $\mathcal{G}_{new}^{\neq n} \leftarrow \left( \begin{array}{c} \boxtimes_2 \\ n+1, \dots, N-1 \end{array} \mathcal{G}_j \right) \boxtimes_2 \mathcal{G}_N^{new} \boxtimes_2 \left( \begin{array}{c} \boxtimes_2 \\ 1, \dots, n-1 \end{array} \mathcal{G}_j \right)$ 
13:    Compute  $(\mathcal{G}_{new}^{\neq n})_S$  and  $\mathbf{X}_{S[n]}^{new}$  using Algorithm 3 or Algorithm 6
14:     $\mathbf{P}_n \leftarrow \mathbf{P}_n + \mathbf{X}_{S[n]}^{new} (\mathcal{G}_{new}^{\neq n})_{S[2]}$ 
15:     $\mathbf{Q}_n \leftarrow \mathbf{Q}_n + (\mathcal{G}_{new}^{\neq n})_{S[2]}^\top (\mathcal{G}_{new}^{\neq n})_{S[2]}$ 
16:     $\mathbf{G}_{n(2)} \leftarrow \mathbf{P}_n \mathbf{Q}_n^\dagger$  and reshape  $\mathbf{G}_{n(2)}$  to  $\mathcal{G}_n$ 
17:  end for
18: end for

```

and $\mathbf{D}_n \in \mathbb{R}^{m \times m}$ is a diagonal rescaling matrix with the i -th diagonal entry $(\mathbf{D}_n)_{ii} = \sqrt{J_n/m}$. In practice, the rescaling matrix can be ignored without affecting the performance of algorithms. Furthermore, the sampling can be carried out in TR-cores as done in Algorithm 3. The detailed algorithm is summarized in Algorithm 7 in Appendix B and the theoretical guarantee is as follows.

Theorem 3.1 Let Ψ_n be a uniform sampling matrix as defined above and

$$\tilde{\mathbf{G}}_{n(2)} \stackrel{\text{def}}{=} \arg \min_{\mathbf{G}_{n(2)}} \left\| \mathbf{X}_{[n]} \Psi_n^\top - \mathbf{G}_{n(2)} (\Psi_n \mathbf{G}_{[2]}^{\neq n})^\top \right\|_F.$$

If

$$m \geq \left(\frac{2\gamma R_n R_{n+1}}{\varepsilon} \right) \max \left[\frac{48}{\varepsilon} \ln \left(\frac{96\gamma R_n R_{n+1}}{\varepsilon^2 \sqrt{\delta}} \right), \frac{1}{\delta} \right]$$

with $\varepsilon \in (0, 1)$, $\delta \in (0, 1)$, and $\gamma > 1$, then the following inequality holds with a probability of at least $1 - \delta$:

$$\left\| \mathbf{X}_{[n]} - \tilde{\mathbf{G}}_{n(2)} (\mathbf{G}_{[2]}^{\neq n})^\top \right\|_F \leq (1 + \varepsilon) \min_{\mathbf{G}_{n(2)}} \left\| \mathbf{X}_{[n]} - \mathbf{G}_{n(2)} (\mathbf{G}_{[2]}^{\neq n})^\top \right\|_F.$$

Remark 3.6 The γ in Theorem 3.1 determines the maximum value of the row norms of the left singular vector matrix of the coefficient matrix $\mathbf{G}_{[2]}^{\neq n}$ (see Theorem A.1). It can be seen that the more inhomogeneous the coefficient matrix is, the larger the γ is, which leads to less effective for uniform sampling. In this case, the importance sampling is a more reasonable choice.

Leverage-based Sampling Two definitions are first introduced.

Definition 3.1 (Leverage Scores [7]) Let $\mathbf{A} \in \mathbb{R}^{m \times n}$ with $m > n$, and let $\mathbf{Q} \in \mathbb{R}^{m \times n}$ be any orthogonal basis for the column space of \mathbf{A} . The **leverage score** of the i -th row of \mathbf{A} is given by

$$\ell_i(\mathbf{A}) = \|\mathbf{Q}(i, :)\|_2^2.$$

Definition 3.2 (Leverage-based Probability Distribution [26]) Let $\mathbf{A} \in \mathbb{R}^{m \times n}$ with $m > n$. We say a probability distribution $\mathbf{q} = [q_1, \dots, q_m]^\top$ is a **leverage-based probability distribution** for \mathbf{A} on $[m]$ if $q_i \geq \beta p_i$ with $p_i = \frac{\ell_i(\mathbf{A})}{n}$, $0 < \beta \leq 1$ and $\forall i \in [m]$.

Computing the leverage scores of $\mathbf{G}_{[2]}^{\neq n} \in \mathbb{R}^{J_n \times R_n R_{n+1}}$ directly is expensive. Fortunately, by [18], we can estimate them using the leverage scores related to the TR-cores $\mathcal{G}_1, \dots, \mathcal{G}_{n-1}, \mathcal{G}_{n+1}, \dots, \mathcal{G}_N$.

Lemma 3.1 ([18]) For each $n \in [N]$, let $\mathbf{p}_n \in \mathbb{R}^{I_n}$ be a probability distribution on $[I_n]$ defined element-wise via

$$\mathbf{p}_n(i_n) = \frac{\ell_{i_n}(\mathbf{G}_{n(2)})}{\text{rank}(\mathbf{G}_{n(2)})},$$

$\mathbf{p}^{\neq n}$ be a probability distribution on $[J_n]$ defined element-wise via

$$\mathbf{p}^{\neq n}(i) = \frac{\ell_i(\mathbf{G}_{[2]}^{\neq n})}{\text{rank}(\mathbf{G}_{[2]}^{\neq n})},$$

$\mathbf{q}^{\neq n}$ be a vector defined element-wise via

$$\mathbf{q}^{\neq n}(\overline{i_{n+1} \cdots i_N i_1 \cdots i_{n-1}}) = \prod_{\substack{m=1 \\ m \neq n}}^N \mathbf{p}_m(i_m),$$

and β_n be a constant as in Definition 3.2 defined as

$$\beta_n = \left(R_n R_{n+1} \prod_{\substack{m=1 \\ m \notin \{n, n+1\}}}^N R_m^2 \right)^{-1}.$$

Then for each $n \in [N]$, $\mathbf{q}^{\neq n}(i) \geq \beta_n \mathbf{p}^{\neq n}(i)$ for all $i = \overline{i_{n+1} \cdots i_N i_1 \cdots i_{n-1}} \in [J_n]$ and hence $\mathbf{q}^{\neq n}$ is the leverage-based probability distribution for $\mathbf{G}_{[2]}^{\neq n}$ on $[J_n]$.

With this lemma, we can define the sampling matrix in (3.6) as follows:

$$(\mathbf{S}_n)_{ij} = \begin{cases} 1, & \text{if the } j\text{-th row is chosen in the } i\text{-th independent random trial} \\ & \text{with the probability } \mathbf{q}^{\neq n}(j), \\ 0, & \text{otherwise,} \end{cases}$$

and the i -th diagonal entry of the diagonal rescaling matrix \mathbf{D}_n in (3.6) is now $(\mathbf{D}_n)_{ii} = 1/\sqrt{m\mathbf{q}^{\neq n}(j)}$. As above, the rescaling matrix can be ignored and the sampling can be carried out in TR-cores as done in Algorithm 3. The detailed algorithm is summarized in Algorithm 8 in Appendix B and the theoretical guarantee is given in the following.

Theorem 3.2 *Let Ψ_n be a leveraged-based sampling matrix as defined above and*

$$\tilde{\mathbf{G}}_{n(2)} \stackrel{\text{def}}{=} \arg \min_{\mathbf{G}_{n(2)}} \left\| \mathbf{X}_{[n]} \Psi_n^\top - \mathbf{G}_{n(2)} (\Psi_n \mathbf{G}_{[2]}^{\neq n})^\top \right\|_F.$$

If

$$m > \left(\prod_{j=1}^N R_j^2 \right) \max \left[\frac{16}{3(\sqrt{2}-1)^2} \ln \left(\frac{4R_n R_{n+1}}{\delta} \right), \frac{4}{\varepsilon \delta} \right]$$

with $\varepsilon \in (0, 1)$ and $\delta \in (0, 1)$, then the following inequality holds with a probability of at least $1 - \delta$:

$$\left\| \mathbf{X}_{[n]} - \tilde{\mathbf{G}}_{n(2)} (\mathbf{G}_{[2]}^{\neq n})^\top \right\|_F \leq (1 + \varepsilon) \min_{\mathbf{G}_{n(2)}} \left\| \mathbf{X}_{[n]} - \mathbf{G}_{n(2)} (\mathbf{G}_{[2]}^{\neq n})^\top \right\|_F.$$

KSRFT The definition of KSRFT is listed as follows.

Definition 3.3 (KSRFT [4, 12]) The KSRFT is defined as

$$\Psi = \sqrt{\frac{\prod_{j=1}^N I_j}{m}} \mathbf{S} \left(\bigotimes_{j=1}^N (\mathbf{F}_j \mathbf{D}_j) \right),$$

where

- $\mathbf{S} \in \mathbb{R}^{m \times \prod_{j=1}^N I_j}$: m rows, drawn uniformly with replacement, of the $\prod_{i=1}^N I_i \times \prod_{j=1}^N I_j$ identity matrix, i.e., it is a uniform sampling matrix;
- $\mathbf{F}_j \in \mathbb{C}^{I_j \times I_j}$: (unitary) discrete Fourier transform (DFT) of dimension I_j ;
- $\mathbf{D}_j \in \mathbb{R}^{I_j \times I_j}$: a diagonal matrix with independent random diagonal entries drawn uniformly from $\{+1, -1\}$ (also called random sign-flip operator).

Algorithm 6 shows the method for calculating the sketched subchain and input tensors based on KSRFT, which is summarized from [30]. Considering

that KSRFT transforms the original TR-ALS subproblems into complex ones, the update of TR-cores needs to do the following slight change:

$$\begin{aligned}\mathbf{G}_{N(2)}^{new} &\leftarrow \Re\left(\hat{\mathbf{X}}_{S[N]}^{new}\right)\left(\Re\left(\left(\hat{\mathbf{G}}_{S[2]}^{\neq N}\right)^\top\right)\right)^\dagger, & \mathbf{G}_{N(2)} &\leftarrow \begin{bmatrix} \mathbf{G}_{N(2)}^{old} \\ \mathbf{G}_{N(2)}^{new} \end{bmatrix}, \\ \mathbf{P}_n &\leftarrow \mathbf{P}_n^{old} + \mathbf{P}_n + \hat{\mathbf{X}}_{S[n]}^{new} \overline{\left(\hat{\mathbf{G}}_{S[2]}^{\neq n}\right)}, \\ \mathbf{Q}_n &\leftarrow \mathbf{Q}_n^{old} + \left(\hat{\mathbf{G}}_{S[2]}^{\neq n}\right)^\top \left(\hat{\mathbf{G}}_{S[2]}^{\neq n}\right), \\ \mathbf{G}_{n(2)} &\leftarrow \Re(\mathbf{P}_n)\Re(\mathbf{Q}_n)^\dagger,\end{aligned}$$

where $\hat{\mathbf{X}} = \mathbf{X} \times_1 (\mathbf{F}_1 \mathbf{D}_1) \times_2 (\mathbf{F}_2 \mathbf{D}_2) \cdots \times_N (\mathbf{F}_N \mathbf{D}_N)$, $\hat{\mathbf{G}}_n = \mathbf{G}_n \times_2 (\mathbf{F}_n \mathbf{D}_n)$ for $n = 1, \dots, N$, and $\Re(\cdot)$ and $\overline{(\cdot)}$ remain the real-value and conjugation of entries of a matrix, respectively. The detailed algorithm is summarized in Algorithm 9 in Appendix B and the theoretical guarantee is given in Theorem 3.3.

Algorithm 6 Sketched subchain and input tensors based on KSRFT, summarized from [30]

Input: TR-cores $\{\mathcal{G}_k \in \mathbb{R}^{R_k \times I_k \times R_{k+1}}\}_{k=1, k \neq n}^N$, sketch size m , tensor mode n

Output: sketched subchain tensor $\hat{\mathcal{G}}_S^{\neq n}$, sketched input tensor $\hat{\mathbf{X}}_{S[n]}$

- 1: Define the random sign-flip operators \mathbf{D}_j and DFT matrices \mathbf{F}_j for $j \in [N]$
 - 2: Mix TR-cores: $\hat{\mathcal{G}}_j \leftarrow \mathcal{G}_j \times_2 (\mathbf{F}_j \mathbf{D}_j)$, for $j \in [N] \setminus n$
 - 3: Mix tensor: $\hat{\mathbf{X}} \leftarrow \mathbf{X} \times_1 (\mathbf{F}_1 \mathbf{D}_1) \times_2 (\mathbf{F}_2 \mathbf{D}_2) \cdots \times_N (\mathbf{F}_N \mathbf{D}_N)$
 - 4: **for** $n = 1, \dots, N$ **do**
 - 5: Define sampling operator $\mathbf{S} \in \mathbb{R}^{m \times \prod_{j \neq n} I_j}$
 - 6: Retrieve idxs from \mathbf{S}
 - 7: Compute $\hat{\mathcal{G}}_S^{\neq n}$ and $\hat{\mathbf{X}}_{S[n]}$ by Algorithm 3 using uniform sampling
 - 8: $\hat{\mathbf{X}}_{S[n]} \leftarrow \mathbf{D}_n \mathbf{F}_n^* \hat{\mathbf{X}}_{S[n]}$
 - 9: **end for**
-

Theorem 3.3 Let Ψ_n be a KSRFT as defined in Definition 3.3 and

$$\tilde{\mathbf{G}}_{n(2)} \stackrel{\text{def}}{=} \arg \min_{\mathbf{G}_{n(2)}} \left\| \mathbf{X}_{[n]} \Psi_n^\top - \mathbf{G}_{n(2)} (\Psi_n \mathbf{G}_{[2]}^{\neq n})^\top \right\|_F.$$

If $m \geq \mathcal{O}(xy)$ with

$$\begin{aligned}x &= \varepsilon^{-1} (R_n R_{n+1}) \log^{2N-3} \left(\left(\frac{R_n R_{n+1}}{\varepsilon} \right)^{\frac{R_n R_{n+1}}{2}} \frac{N-1}{\eta} \right), \\ y &= \log^4 \left(\left(\frac{R_n R_{n+1}}{\varepsilon} \right)^{\frac{1}{2}} \log^{N-1} \left(\left(\frac{R_n R_{n+1}}{\varepsilon} \right)^{\frac{R_n R_{n+1}}{2}} \frac{N-1}{\eta} \right) \right) \log \prod_{j \neq n} I_j,\end{aligned}$$

where $\varepsilon \in (0, 1)$ is such that $\prod_{j \neq n} I_j \lesssim 1/\varepsilon^{R_n R_{n+1}}$ with $R_n R_{n+1} \geq 2$, $\delta \in (0, 1)$, and $\eta \in (0, 1)$, then the following inequality holds with a probability of at least $1 - \eta - 2^{-\Omega(\log \prod_{j \neq n} I_j)}$:

$$\left\| \mathbf{X}_{[n]} - \tilde{\mathbf{G}}_{n(2)}(\mathbf{G}_{[2]}^{\neq n})^\top \right\|_F \leq (1 + \varepsilon) \min_{\mathbf{G}_{n(2)}} \left\| \mathbf{X}_{[n]} - \mathbf{G}_{n(2)}(\mathbf{G}_{[2]}^{\neq n})^\top \right\|_F.$$

Furthermore, if an assumption on $(N - 1)/\eta \leq (R_n R_{n+1}/\varepsilon)^{R_n R_{n+1}/2}$ also holds, the bound on sketch size can be changed to

$$m \geq \mathcal{O} \left(\varepsilon^{-1(R_n R_{n+1})^{2(N-1)} \log^{2N-3} \left(\frac{R_n R_{n+1}}{\varepsilon} \right)} \log^4 \left(\frac{R_n R_{n+1}}{\varepsilon} \log \left(\frac{R_n R_{n+1}}{\varepsilon} \right) \right) \log \prod_{j \neq n} I_j \right).$$

4 Numerical Experiments

In this section, we consider the numerical performance of our STR and rSTR¹. Specifically, we first examine their effectiveness and efficiency on two real-world datasets. Then, based on the investigation on synthetic tensors, we show their performance from various perspectives in greater detail. Six baselines have been chosen as competitors to evaluate the performance in our experiments:

- TR-ALS (Cold) [34]: an implementation of TR-ALS without special initialization.
- TR-ALS (Hot): the same as above but the TR decomposition of the last time step is used as the initialization for decomposing the current tensor.
- TR-ALS-NE [29]: a practical implementation of TR-ALS.
- TR-ALS-Sampled-U: a sampling-based algorithm with uniform sampling.
- TR-ALS-Sampled [18]: the same as above but with leverage-based sampling.
- TR-KSRFT-ALS [30]: a practical implementation of KSRFT-based algorithm.

The computational complexities of the above methods as well as ours are listed in Table 4.1. In addition, our STR and rSTR occupy the memory space of

$$I^{N-1} t^{new} + (2(N-1)I + t^{old})R^2 + (N-1)R^4,$$

which is much smaller than $I^{N-1}(t^{old} + t^{new})$, the memory space of the other methods.

The experimental protocol is the same for all the experiments. Specifically, for a given dataset of size $I_1 \times \cdots \times I_N$, a subtensor of size $I_1 \times \cdots \times I_{N-1} \times (20\%I_N)$ is first decomposed by TR-ALS and the TR decomposition is used to initialize all the algorithms. After that, a section of size $I_1 \times \cdots \times I_{N-1} \times t^{new}$ of the remaining data is appended to the existing tensor at a time step, immediately following which all the methods record their processing time for

¹ We use rSTR-U, rSTR-L and rSTR-K to notate rSTR with uniform sampling, leverage-based sampling and KSRFT, respectively.

Table 4.1: Complexity comparison of various algorithms (Ignoring the initialization, i.e., the initial TR-cores in offline algorithms and the initialization stage in STR and rSTR, and setting $\mathbf{X} \in \mathbb{R}^{I \times \dots \times I \times (t^{old} + t^{new})}$ with the target TR-ranks $R_1 = \dots = R_N = R$ satisfying $R^2 < I$).

Method	Time only for one time step
TR-ALS	$\mathcal{O}(\#it \cdot NI^{N-1}R^2(t^{old} + t^{new}))$ // #it denotes the number of outer loop iterations
TR-ALS-NE	$\mathcal{O}((N-1)IR^4 + (t^{old} + t^{new})R^4 + \#it \cdot NI^{N-1}R^2(t^{old} + t^{new}))$
TR-ALS-Sampled-U	$\mathcal{O}(\#it \cdot ((N-1)ImR^2 + (t^{old} + t^{new})mR^2))$
TR-ALS-Sampled	$\mathcal{O}((N-1)IR^4 + (t^{old} + t^{new})R^4 + \#it \cdot ((N-1)ImR^2 + (t^{old} + t^{new})mR^2))$
TR-KSRFT-ALS	$\mathcal{O}(I^{N-1}(t^{old} + t^{new}) \log(I^{N-1}(t^{old} + t^{new}))) + \#it \cdot ((N-1)ImR^2 + (t^{old} + t^{new})mR^2))$
STR	$\mathcal{O}(NI^{N-1}R^2t^{new})$
rSTR-U	$\mathcal{O}((N-1)ImR^2 + t^{new}mR^2)$
rSTR-L	$\mathcal{O}((N-1)ImR^2 + t^{new}mR^2)$
rSTR-K	$\mathcal{O}(I^{N-1}(t^{new}) \log(I^{N-1}(t^{new})))$

this step, as well as calculate the relative errors of their current decompositions by

$$\frac{\|\mathbf{X} - \hat{\mathbf{X}}\|_F}{\|\mathbf{X}\|_F} = \frac{\|\mathbf{X} - \text{TR}(\{\hat{\mathbf{G}}_n\}_{n=1}^N)\|_F}{\|\mathbf{X}\|_F},$$

where the TR-cores $\{\hat{\mathbf{G}}_n\}_{n=1}^N$ are computed by various algorithms. Thus, continuing the process, we can report and compare the processing time and relative errors for all the time steps.

The same experiment is replicated 10 times for all datasets by using Matlab R2022a on a computer with an Intel Xeon W-2255 3.7 GHz CPU, and 256 GB RAM, and the final results are averaged over these runs. Additionally, we also use the Matlab Tensor Toolbox [3].

For the initialization stage, there are some settings of parameters that need to be clarified. Firstly, since we only care about the comparison on relative performance among different algorithms, it is not necessary to pursue the best rank decomposition for each dataset. Hence, unless otherwise stated, the target rank R is always fixed to 5 for all the datasets. Secondly, to find a good initial TR decomposition, the tolerance ϵ (the value of the change in relative error between two adjacent steps) is set to $1e-8$ and the maximum number of iterations IT is set to 100. Note that the performance of online algorithms depends on the quality of the initial decomposition [35, 16]. However, exploring the impact of initialization is not our main purpose. So, we use the same initialization for both STR and rSTR. Whereas, in practice, it is better to validate the goodness of the initialization to obtain the best subsequent effectiveness.

In addition, in terms of method-specific parameters, for the six batch algorithms (i.e., the six baselines), the default settings, $\epsilon = 1e-10$ and $IT = 50$, are used, and we adopt the same sketch size $m = 1000$ in all the randomized algorithms, which has little effect on experiments except for Figure 4.5, since the rank is changing there. Besides, unless otherwise stated, we always set $t^{new} = 5$ for all the datasets.

4.1 Effectiveness and efficiency

The experiments are conducted on two real-world datasets of varying characteristics and higher-order structure. Specifically, we extract 360 gray-scale images from the popular image dataset *Columbia Object Image Library (COIL-20)*² to form a tensor of size $416 \times 448 \times 360$ and 300 frames of a popular video sequences from *Hall*³ to form a tensor of size $144 \times 176 \times 3 \times 300$.

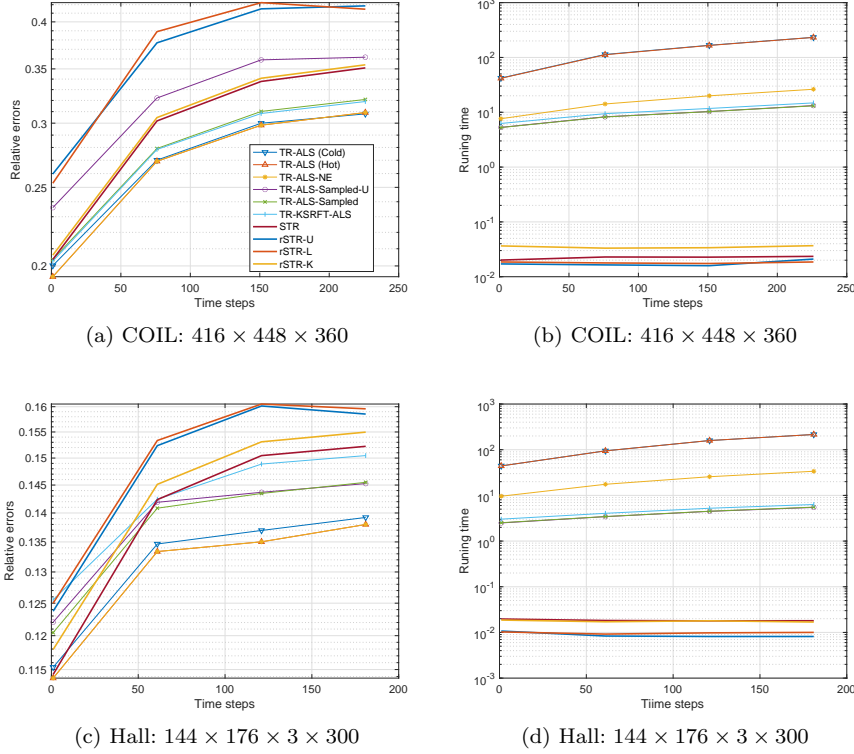


Fig. 4.1: Time steps v.s. Relative errors and Time steps v.s. Running time output by algorithms for two real-world datasets.

For these two tensors, the relative errors and processing time for each time step of various algorithms are reported in Figure 4.1, from which we can see that the batch methods, i.e., TR-ALS, TR-ALS-NE, TR-ALS-Sampled-U, TR-ALS-Sampled and TR-KSRFT-ALS, have the expected results which we have known from [30,29]. That is, TR-ALS-NE is identical to TR-ALS in terms

² <https://cave.cs.columbia.edu/repository/COIL-20>

³ <https://github.com/qbzhao/BRTF/tree/master/videos>

of accuracy, but takes much less time due to the structure being used in the algorithm; the three randomized algorithms can accelerate the deterministic methods, however, loss some accuracy. In addition, TR-ALS (Cold) is slightly less accurate than TR-ALS (Hot). The main reason is that using previous results as initialization can provide a descending seed point for the ALS algorithm, while TR-ALS (Cold) discards this useful information completely.

Our proposed algorithms, i.e., STR and rSTR, show very promising results in terms of accuracy and speed. Specifically, STR is fairly consistent and very similar to the batch methods in accuracy; rSTR performs slightly worse but the differences are not remarkable. However, both of them are much faster than all the batch methods including the randomized ones. Comparing STR and rSTR, the sampling-based rSTR, i.e., rSTR-U and rSTR-L, shows an advantage in computing time, however, the projection-based rSTR, i.e., rSTR-K, is not very competitive in this respect. The main reason is that an expensive step, i.e., the mixing tensor step, needs to be performed at each time step; see [30] for more details. While, when the tensor order increases, the advantage of rSTR-K in running time will gradually emerge; see the experiments in Section 4.2 below.

4.2 More comparisons

In this subsection, with the synthetic data formed by TR decomposition whose TR-cores are generated by random Gaussian tensors with entries drawn independently from a standard normal distribution, we show the impact on performance of various parameters appearing in the computational complexities of algorithms; see Table 4.1 for the specific complexities. More specifically, we compare each algorithm by varying five parameters: the order (N), the dimension (I), the dimension of the temporal mode (I_N), the temporal slice size (t^{new}), and the rank ($R_{true} = R$).

We first vary N and I . Numerical results on decomposition for four tensors with different orders and dimensions are given in Figure 4.2, which shows the similar results to the previous experiments in Section 4.1. This further validates the effectiveness and efficiency of our algorithms. Note that TR-ALS (Cold) may fluctuate wildly. This is because, as explained above, reinitialization may lead the method to be nonstable.

Now, we vary I_N . Specifically, we set $\mathcal{X} : 30 \times 30 \times 30 \times 30 \times I_N$ with $I_N = 120, 140, 160, 180, 200$. The final relative errors and the total running time for each tensor are measured and displayed in Figure 4.3, and we can see that, with the errors being almost unchanged, the complexities for all the algorithms increase as the length of processed data grows as expected.

Thirdly, we consider the tensor $\mathcal{X} : 30 \times 30 \times 30 \times 30 \times 200$ with $t^{new} = 2, 4, 6, 8, 10$ and record the final relative errors and the total running time when the whole tensor is decomposed. As can be seen from Figure 4.4, the temporal slice size has little effect on the quality of the decomposition, but in terms of running time, the larger the temporal slice size is, the less the total running time is. This is because, for a tensor with a fixed time dimension,

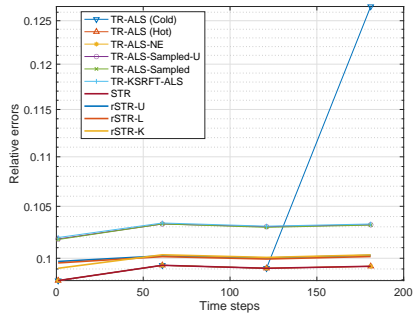
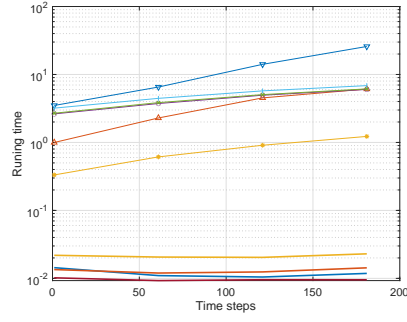
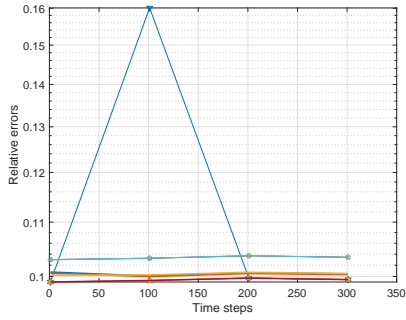
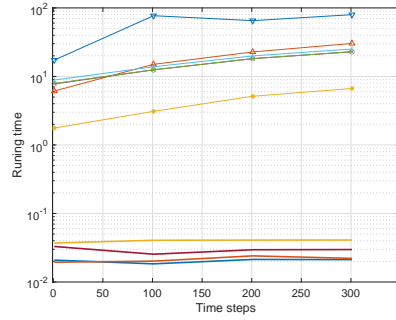
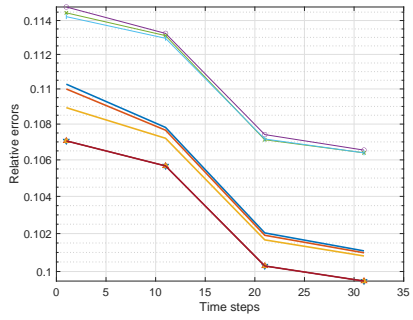
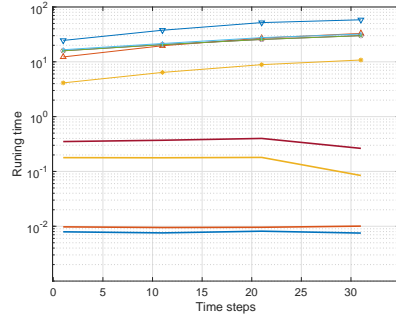
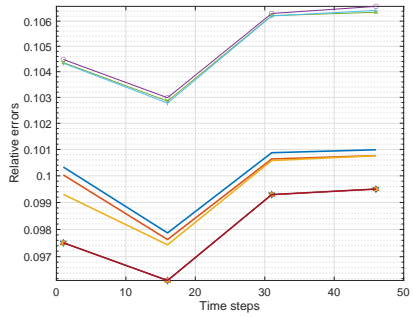
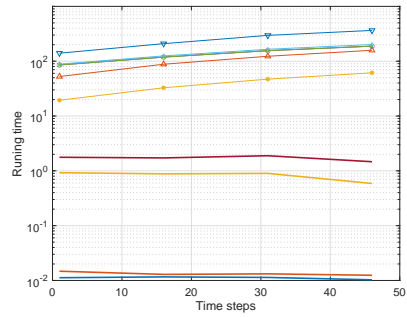
(a) $\mathcal{X} : 300 \times 300 \times 300$ (b) $\mathcal{X} : 300 \times 300 \times 300$ (c) $\mathcal{X} : 500 \times 500 \times 500$ (d) $\mathcal{X} : 500 \times 500 \times 500$ (e) $\mathcal{X} : 40 \times 40 \times 40 \times 40 \times 40$ (f) $\mathcal{X} : 40 \times 40 \times 40 \times 40 \times 40$ (g) $\mathcal{X} : 60 \times 60 \times 60 \times 60 \times 60$ (h) $\mathcal{X} : 60 \times 60 \times 60 \times 60 \times 60$

Fig. 4.2: Time steps v.s. Relative errors and Time steps v.s. Running time output by algorithms for tensors with different orders and dimensions.

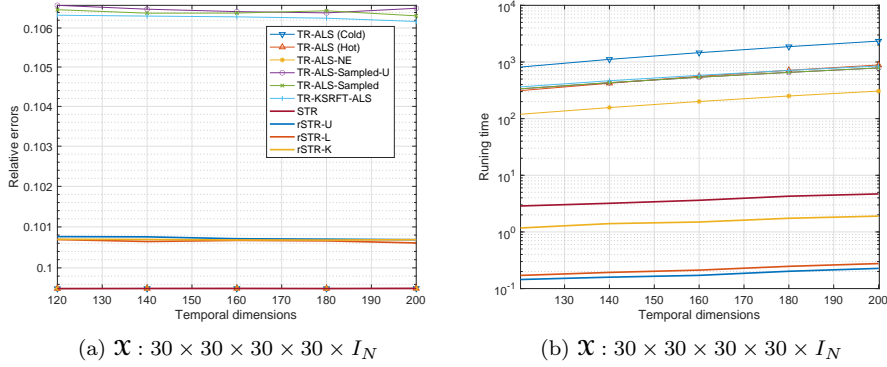


Fig. 4.3: Temporal dimensions v.s. Relative errors and Temporal dimensions v.s. Running time output by algorithms for tensors with different temporal dimensions $I_N = 120, 140, 160, 180, 200$.

larger temporal slice size means fewer time steps and hence less running time.

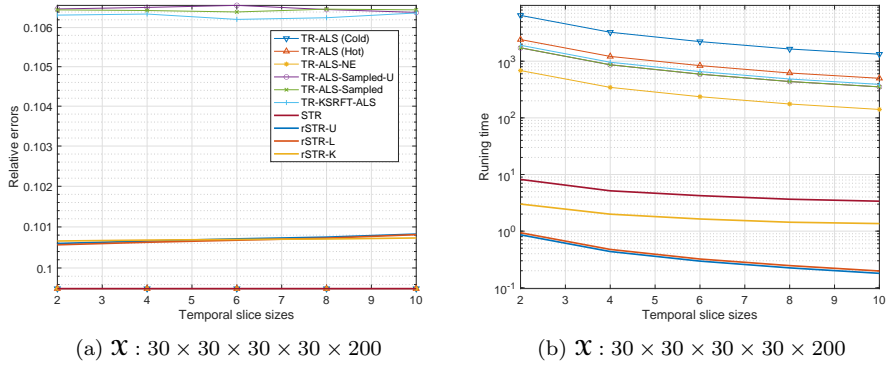


Fig. 4.4: Temporal slice sizes v.s. Relative errors and Temporal slice sizes v.s. Running time output by algorithms for a tensor with different temporal slice sizes $t^{new} = 2, 4, 6, 8, 10$.

Finally, we vary the rank $R_{true} = R$ for tensors $\mathcal{X} : 30 \times 30 \times 30 \times 30 \times 200$. The final relative errors and the total running time for $R = 3, 4, 5, 6$ are reported in Figure 4.5, from which it is seen that the relative errors for STR and three offline deterministic algorithms, i.e., TR-ALS (Cold), TR-ALS (Hot), TR-ALS-NE, have no change as R varies. Whereas, for randomized algorithms, the errors will increase with the rank growing. This is because, by

Theorems 3.1 to 3.3, the sketch size of randomized algorithms is related to the size of the rank, while the former is fixed in our experiments. In comparison, the range of change for our rSTR is smaller, which is mainly due to the use of the better decomposition results from the previous time step. As for the running time, all the randomized algorithms hardly varies as the rank increases, while several deterministic methods increase a little. This is not well reflected in Table 4.1 because the assumptions there are not satisfied when the rank increases, thus making the overall leading order complexity change.

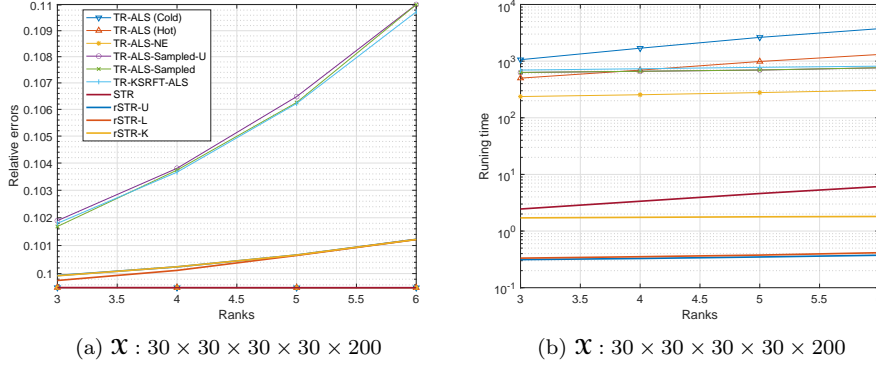


Fig. 4.5: Ranks v.s. Relative errors and Ranks v.s. Running time output by algorithms for tensors with different ranks $R_{true} = R = 3, 4, 5, 6$.

5 Concluding Remarks

This paper discusses the problem of tracking TR decompositions of streaming tensors. A streaming algorithm, i.e., STR, is first proposed that can efficiently monitor the new decomposition by employing complementary TR-cores to temporally store the valuable information from the previous time step. Then, we provide a randomized variant of STR, i.e., rSTR, which can permit various randomization techniques conveniently and cheaply due to the use of the structure of the coefficient matrices in TR-ALS. Numerical results on both real-world and synthetic datasets demonstrate that our algorithms are comparable to the accurate batch methods in accuracy, and outperform them considerably in terms of computational cost.

There is some room for methodological improvement. By incorporating numerous popular regularizers and constraints, such as nonnegativity, we can further increase the adaptability of our methods, making them more suited for applications such as computer vision. Moreover, our algorithms presume that the rank of TR decomposition remains constant throughout the streaming process. Increasing TR-ranks in streaming TR decompositions is a viable

option. In addition, it is also valuable to extend our methods to accommodate streaming tensors that can be modified in any mode, i.e., multi-aspect streaming tensors.

Declarations

Data Availability

The data that support the findings of this study are available from the corresponding author upon reasonable request.

Competing Interests

The authors declare that they have no conflict of interest.

References

1. Ahmadi-Asl, S., Caiafa, C.F., Cichocki, A., Phan, A.H., Tanaka, T., Oseledets, I., Wang, J.: Cross tensor approximation methods for compression and dimensionality reduction. *IEEE Access* **9**, 150809–150838 (2021). DOI 10.1109/ACCESS.2021.3125069
2. Ahmadi-Asl, S., Cichocki, A., Phan, A.H., Asante-Mensah, M.G., Ghazani, M.M., Tanaka, T., Oseledets, I.V.: Randomized algorithms for fast computation of low rank tensor ring model. *Mach. Learn.: Sci. Technol.* **2**(1), 011001 (2020). DOI 10.1088/2632-2153/abad87
3. Bader, B.W., Kolda, T.G., et al.: Tensor toolbox for matlab (2021). URL <https://www.tensortoolbox.org>. Version 3.2.1
4. Battaglino, C., Ballard, G., Kolda, T.G.: A practical randomized CP tensor decomposition. *SIAM J. Matrix Anal. Appl.* **39**(2), 876–901 (2018). DOI 10.1137/17M1112303
5. Chachlakis, D.G., Dhanaraj, M., Prater-Bennette, A., Markopoulos, P.P.: Dynamic 11-norm tucker tensor decomposition. *IEEE J. Sel. Topics Signal Process.* **15**(3), 587–602 (2021). DOI 10.1109/JSTSP.2021.3058846
6. Drineas, P., Kannan, R., Mahoney, M.W.: Fast monte carlo algorithms for matrices i: Approximating matrix multiplication. *SIAM J. Comput.* **36**(1), 132–157 (2006). DOI 10.1137/S0097539704442684
7. Drineas, P., Magdon-Ismail, M., Mahoney, M.W., Woodruff, D.P.: Fast approximation of matrix coherence and statistical leverage. *J. Mach. Learn. Res.* **13**(1), 3475–3506 (2012)
8. Drineas, P., Mahoney, M.W., Muthukrishnan, S., Sarlós, T.: Faster least squares approximation. *Numer. Math.* **117**(2), 219–249 (2011). DOI 10.1007/s00211-010-0331-6
9. Espig, M., Naraparaju, K.K., Schneider, J.: A note on tensor chain approximation. *Comput. Visual Sci.* **15**, 331–344 (2012). DOI 10.1007/s00791-014-0218-7
10. He, Y., Atia, G.K.: Patch tracking-based streaming tensor ring completion for visual data recovery. *IEEE Trans. Circuits Syst. Video Technol.* **32**(12), 8312–8326 (2022). DOI 10.1109/TCSVT.2022.3190818
11. Huang, Z., Qiu, Y., Yu, J., Zhou, G.: Multi-aspect streaming tensor ring completion for dynamic incremental data. *IEEE Signal Process. Lett.* **29**, 2657–2661 (2022). DOI 10.1109/LSP.2022.3231469
12. Jin, R., Kolda, T.G., Ward, R.: Faster Johnson-Lindenstrauss transforms via Kronecker products. *Inf. Inference* **10**(4), 1533–1562 (2021). DOI 10.1093/imaiai/iaaa028
13. Kolda, T.G., Bader, B.W.: Tensor decompositions and applications. *SIAM Rev.* **51**(3), 455–500 (2009). DOI 10.1137/07070111X

14. Kressner, D., Vandereycken, B., Voorhaar, R.: Streaming tensor train approximation. arXiv preprint arXiv:2208.02600 (2022)
15. Liu, H., Yang, L.T., Guo, Y., Xie, X., Ma, J.: An incremental tensor-train decomposition for cyber-physical-social big data. *IEEE Trans. Big Data* **7**(2), 341–354 (2021). DOI 10.1109/TBDATA.2018.2867485
16. Ma, C., Yang, X., Wang, H.: Randomized online CP decomposition. In: 2018 Tenth International Conference on Advanced Computational Intelligence (ICACI), pp. 414–419. IEEE, Xiamen, China (2018)
17. Malik, O.A.: More efficient sampling for tensor decomposition with worst-case guarantees. In: Proceedings of the 39th International Conference on Machine Learning, vol. 162, pp. 14887–14917. PMLR, Virtual Event (2022)
18. Malik, O.A., Becker, S.: A sampling-based method for tensor ring decomposition. In: Proceedings of the 38th International Conference on Machine Learning, vol. 139, pp. 7400–7411. PMLR, Virtual Event (2021)
19. Mickelin, O., Karaman, S.: On algorithms for and computing with the tensor ring decomposition. *Numer. Linear Algebra Appl.* **27**(3), e2289 (2020). DOI 10.1002/nla.2289
20. Oseledets, I.V.: Tensor-train decomposition. *SIAM J. Sci. Comput.* **33**(5), 2295–2317 (2011). DOI 10.1137/090752286
21. Sun, J., Tao, D., Faloutsos, C.: Beyond streams and graphs: Dynamic tensor analysis. In: Proceedings of the 12th ACM SIGKDD International Conference on Knowledge Discovery and Data Mining, vol. KDD '06, pp. 374–383. Association for Computing Machinery, New York, NY, USA (2006)
22. Sun, J., Tao, D., Papadimitriou, S., Yu, P.S., Faloutsos, C.: Incremental tensor analysis: Theory and applications. *ACM Trans. Knowl. Discov. Data* **2**(3), 1556–4681 (2008). DOI 10.1145/1409620.1409621
23. Sun, Y., Guo, Y., Luo, C., Tropp, J., Udell, M.: Low-rank tucker approximation of a tensor from streaming data. *SIAM J. Math. Data Sci.* **2**(4), 1123–1150 (2020). DOI 10.1137/19M1257718
24. Thanh, L.T., Abed-Meraim, K., Trung, N.L., Boyer, R.: Adaptive algorithms for tracking tensor-train decomposition of streaming tensors. In: 2020 28th European Signal Processing Conference (EUSIPCO), pp. 995–999. IEEE, Amsterdam, Netherlands (2021)
25. Thanh, L.T., Abed-Meraim, K., Trung, N.L., Hafiane, A.: A contemporary and comprehensive survey on streaming tensor decomposition. *IEEE Trans. Knowl. Data Eng.* pp. 1–20 (2022). DOI 10.1109/TKDE.2022.3230874
26. Woodruff, D.P.: Sketching as a tool for numerical linear algebra. *Found. Trends Theor. Comput. Sci.* **10**(1–2), 1–157 (2014). DOI 10.1561/04000000060
27. Xiao, H., Wang, F., Ma, F., Gao, J.: eOTD: An efficient online Tucker decomposition for higher order tensors. In: 2018 IEEE International Conference on Data Mining (ICDM), pp. 1326–1331 (2018)
28. Yu, J., Zou, T., Zhou, G.: Online subspace learning and imputation by tensor-ring decomposition. *Neural Netw.* **153**, 314–324 (2022). DOI 10.1016/j.neunet.2022.05.023
29. Yu, Y., Li, H.: Practical alternating least squares for tensor ring decomposition. arXiv preprint arXiv:2210.11362 (2022)
30. Yu, Y., Li, H.: Practical sketching-based randomized tensor ring decomposition. arXiv preprint arXiv:2209.05647 (2022)
31. Yuan, L., Cao, J., Zhao, X., Wu, Q., Zhao, Q.: Higher-dimension tensor completion via low-rank tensor ring decomposition. In: 2018 Asia-Pacific Signal and Information Processing Association Annual Summit and Conference (APSIPA ASC), pp. 1071–1076. IEEE, Honolulu, HI, USA (2018)
32. Yuan, L., Li, C., Cao, J., Zhao, Q.: Randomized tensor ring decomposition and its application to large-scale data reconstruction. In: ICASSP 2019 - 2019 IEEE International Conference on Acoustics, Speech and Signal Processing (ICASSP), pp. 2127–2131. IEEE, Brighton Conference Centre Brighton, U.K. (2019)
33. Zeng, C., Ng, M.K.: Incremental CP tensor decomposition by alternating minimization method. *SIAM J. Matrix Anal. Appl.* **42**(2), 832–858 (2021). DOI 10.1137/20M1319097
34. Zhao, Q., Zhou, G., Xie, S., Zhang, L., Cichocki, A.: Tensor ring decomposition. arXiv preprint arXiv:1606.05535 (2016)

35. Zhou, S., Vinh, N.X., Bailey, J., Jia, Y., Davidson, I.: Accelerating online CP decompositions for higher order tensors. In: Proceedings of the 22nd ACM SIGKDD International Conference on Knowledge Discovery and Data Mining, vol. KDD '16, pp. 1375–1384. Association for Computing Machinery, New York, NY, USA (2016)

Appendix

A Proofs

We first state some preliminaries that will be used in the proofs, where Lemma A.1 is a variant of [8, Lemma 1] for multiple right hand sides, Lemma A.2 is a part of [6, Lemma 8], and Lemma A.3 is from [8, Theorem 4].

Lemma A.1 Let $\text{OPT} \stackrel{\text{def}}{=} \min_{\mathbf{X}} \|\mathbf{A}\mathbf{X} - \mathbf{Y}\|_F$ with $\mathbf{A} \in \mathbb{R}^{I \times R}$ and $I > R$, let $\mathbf{U} \in \mathbb{R}^{I \times \text{rank}(\mathbf{A})}$ contain the left singular vectors of \mathbf{A} , let \mathbf{U}^\perp be an orthogonal matrix whose columns span the space perpendicular to $\text{range}(\mathbf{U})$ and define $\mathbf{Y}^\perp \stackrel{\text{def}}{=} \mathbf{U}^\perp (\mathbf{U}^\perp)^\top \mathbf{Y}$. If $\Psi \in \mathbb{R}^{m \times I}$ satisfies

$$\sigma_{\min}^2(\Psi\mathbf{U}) \geq \frac{1}{\sqrt{2}}, \quad (\text{A.1})$$

$$\|\mathbf{U}^\top \Psi^\top \Psi \mathbf{Y}^\perp\|_F^2 \leq \frac{\varepsilon}{2} \text{OPT}^2, \quad (\text{A.2})$$

for some $\varepsilon \in (0, 1)$, then

$$\|\mathbf{A}\tilde{\mathbf{X}} - \mathbf{Y}\|_F \leq (1 + \varepsilon) \text{OPT},$$

where $\tilde{\mathbf{X}} \stackrel{\text{def}}{=} \arg \min_{\mathbf{X}} \|\Psi\mathbf{A}\mathbf{X} - \Psi\mathbf{Y}\|_F$.

Lemma A.2 Let \mathbf{A} and \mathbf{B} be matrices with I rows, and let $\mathbf{q} \in \mathbb{R}^I$ be a probability distribution satisfying

$$\mathbf{q}(i) \geq \beta \frac{\|\mathbf{A}(i, \cdot)\|_2^2}{\|\mathbf{A}\|_F^2} \text{ for all } i \in [I] \text{ and some } \beta \in (0, 1].$$

If $\Psi \in \mathbb{R}^{m \times I}$ is a sampling matrix with the probability distribution \mathbf{q} , then

$$\mathbb{E} \|\mathbf{A}^\top \mathbf{B} - \mathbf{A}^\top \Psi^\top \Psi \mathbf{B}\|_F^2 \leq \frac{1}{\beta m} \|\mathbf{A}\|_F^2 \|\mathbf{B}\|_F^2.$$

Lemma A.3 Let $\mathbf{A} \in \mathbb{R}^{I \times R}$ with $\|\mathbf{A}\|_2 \leq 1$, and let $\mathbf{q} \in \mathbb{R}^I$ be a probability distribution satisfying

$$\mathbf{q}(i) \geq \beta \frac{\|\mathbf{A}(i, \cdot)\|_2^2}{\|\mathbf{A}\|_F^2} \text{ for all } i \in [I] \text{ and some } \beta \in (0, 1].$$

If $\Psi \in \mathbb{R}^{m \times I}$ is a sampling matrix with the probability distribution \mathbf{q} , $\varepsilon \in (0, 1)$ is an accuracy parameter, $\|\mathbf{A}\|_F^2 \geq \frac{1}{24}$, and

$$m \geq \frac{96 \|\mathbf{A}\|_F^2}{\beta \varepsilon^2} \ln \left(\frac{96 \|\mathbf{A}\|_F^2}{\beta \varepsilon^2 \sqrt{\delta}} \right),$$

then, with a probability of at least $1 - \delta$,

$$\|\mathbf{A}^\top \mathbf{A} - \mathbf{A}^\top \Psi^\top \Psi \mathbf{A}\|_F^2 \leq \varepsilon.$$

A.1 Proof of Theorem 3.1

We first state a theorem similar to [18, Theorem 7], i.e., the theoretical guarantee of uniform sampling for TR-ALS.

Theorem A.1 *Let Ψ_n be a uniform sampling matrix defined as in (3.6), and*

$$\tilde{\mathbf{G}}_{n(2)} \stackrel{\text{def}}{=} \arg \min_{\mathbf{G}_{n(2)}} \left\| \mathbf{X}_{[n]} \Psi_n^\top - \mathbf{G}_{n(2)} (\Psi_n \mathbf{G}_{[2]}^{\neq n})^\top \right\|_F.$$

If

$$m \geq \left(\frac{2\gamma R_n R_{n+1}}{\varepsilon} \right) \max \left[\frac{48}{\varepsilon} \ln \left(\frac{96\gamma R_n R_{n+1}}{\varepsilon^2 \sqrt{\delta}} \right), \frac{1}{\delta} \right],$$

with $\varepsilon \in (0, 1)$, $\delta \in (0, 1)$, and $\gamma > 1$, then the following inequality holds with a probability of at least $1 - \delta$:

$$\left\| \mathbf{X}_{[n]} - \tilde{\mathbf{G}}_{n(2)} (\mathbf{G}_{[2]}^{\neq n})^\top \right\|_F \leq (1 + \varepsilon) \min_{\mathbf{G}_{n(2)}} \left\| \mathbf{X}_{[n]} - \mathbf{G}_{n(2)} (\mathbf{G}_{[2]}^{\neq n})^\top \right\|_F.$$

Proof Let $\mathbf{U} \in \mathbb{R}^{J_n \times \text{rank}(\mathbf{G}_{[2]}^{\neq n})}$ contain the left singular vectors of $\mathbf{G}_{[2]}^{\neq n}$ and $\text{rank}(\mathbf{G}_{[2]}^{\neq n}) = R_n R_{n+1}$. Then, there is a $\gamma > 1$ such that

$$\|\mathbf{U}(i, :)\|_2^2 \leq \frac{\gamma R_n R_{n+1}}{J_n} \quad \text{for all } i \in [J_n]. \quad (\text{A.3})$$

Note that $\|\mathbf{U}\|_F = \sqrt{R_n R_{n+1}}$. Thus, setting $\beta = \frac{1}{\gamma}$, we have

$$\frac{1}{J_n} \geq \beta \frac{\|\mathbf{U}(i, :)\|_2^2}{\|\mathbf{U}\|_F^2}. \quad (\text{A.4})$$

That is, the uniform probability distribution \mathbf{q} on $[J_n]$ satisfies (A.4). Moreover, it is easy to see that $\|\mathbf{U}\|_2 = 1 \leq 1$, $\|\mathbf{U}\|_F^2 = R_n R_{n+1} > \frac{1}{24}$, and

$$m \geq \frac{96 R_n R_{n+1}}{\beta \varepsilon^2} \ln \left(\frac{96 R_n R_{n+1}}{\beta \varepsilon^2 \sqrt{\delta_1}} \right).$$

Thus, noting that Ψ_n is a sampling matrix with the probability distribution \mathbf{q} , applying Lemma A.3 implies that

$$\|\mathbf{U}^\top \mathbf{U} - \mathbf{U}^\top \Psi_n^\top \Psi_n \mathbf{U}\|_2 \leq \varepsilon.$$

On the other hand, note that for all $i \in [R_n R_{n+1}]$,

$$\begin{aligned} |1 - \sigma_i^2(\Psi_n \mathbf{U})| &= |\sigma_i(\mathbf{U}^\top \mathbf{U}) - \sigma_i(\mathbf{U}^\top \Psi_n^\top \Psi_n \mathbf{U})| \\ &\leq \|\mathbf{U}^\top \mathbf{U} - \mathbf{U}^\top \Psi_n^\top \Psi_n \mathbf{U}\|_2. \end{aligned}$$

Thus, choosing $\varepsilon = 1 - 1/\sqrt{2}$ gives that $\sigma_{\min}^2(\Psi_n \mathbf{U}) \geq \frac{1}{\sqrt{2}}$, therefore (A.1) is satisfied.

Next, we check (A.2). Recall that $(\mathbf{X}_{[n]}^\top)^\perp \stackrel{\text{def}}{=} \mathbf{U}^\perp (\mathbf{U}^\perp)^\top \mathbf{X}_{[n]}^\top$. Hence, $\mathbf{U}^\top (\mathbf{X}_{[n]}^\top)^\perp = 0$ and

$$\|(\Psi_n \mathbf{U})^\top \Psi_n (\mathbf{X}_{[n]}^\top)^\perp\|_2^2 = \|\mathbf{U}^\top \Psi_n^\top \Psi_n (\mathbf{X}_{[n]}^\top)^\perp - \mathbf{U}^\top (\mathbf{X}_{[n]}^\top)^\perp\|_2^2.$$

Thus, noting (A.3) and (A.4), applying Lemma A.2, we get

$$\mathbb{E} \left[\|(\Psi_n \mathbf{U})^\top \Psi_n (\mathbf{X}_{[n]}^\top)^\perp\|_2^2 \right] \leq \frac{1}{\beta m} \|\mathbf{U}\|_F^2 \|(\mathbf{X}_{[n]}^\top)^\perp\|_2^2 = \frac{R_n R_{n+1} \text{OPT}^2}{\beta m},$$

where $\text{OPT} = \min_{\mathbf{G}_{n(2)}} \left\| \mathbf{G}_{[2]}^{\neq n} \mathbf{G}_{n(2)}^\top - \mathbf{X}_{[n]}^\top \right\|_F$. Markov's inequality now implies that with probability at least $1 - \delta_2$

$$\|(\Psi_n \mathbf{U})^\top \Psi_n (\mathbf{X}_{[n]}^\top)^\perp\|_2^2 \leq \frac{R_n R_{n+1} \text{OPT}^2}{\delta_2 \beta m}.$$

Setting $m \geq \frac{2R_n R_{n+1}}{\delta_2 \beta \varepsilon}$ and using the value of β specified above, we have that (A.2) is indeed satisfied.

Finally, using Lemma A.1 concludes the proof of the theorem. \square

Proof of Theorem 3.1 For the temporal mode N , if

$$\begin{aligned} \tilde{m}_1 &\geq \left(\frac{2\gamma R_N R_1}{\tilde{\varepsilon}_1} \right) \max \left[\frac{48}{\tilde{\varepsilon}_1} \ln \left(\frac{96\gamma R_N R_1}{\tilde{\varepsilon}_1^2 \sqrt{\delta}} \right), \frac{1}{\delta} \right], \\ \tilde{m}_2 &\geq \left(\frac{2\gamma R_N R_1}{\tilde{\varepsilon}_2} \right) \max \left[\frac{48}{\tilde{\varepsilon}_2} \ln \left(\frac{96\gamma R_N R_1}{\tilde{\varepsilon}_2^2 \sqrt{\delta}} \right), \frac{1}{\delta} \right], \\ &\dots \end{aligned}$$

according to Theorem A.1, at each time step we can obtain a corresponding upper error bound between the new coming tensor and its decomposition as follows

$$\text{The 1st time step: } \left\| \mathbf{X}_{[N]}^{old} - \tilde{\mathbf{G}}_{N(2)}^{old}(\mathbf{G}_{[2]}^{\neq N})^\top \right\|_F \leq (1 + \tilde{\varepsilon}_1) \min_{\mathbf{G}_{N(2)}^{old}} \left\| \mathbf{X}_{[N]}^{old} - \mathbf{G}_{N(2)}^{old}(\mathbf{G}_{[2]}^{\neq N})^\top \right\|_F,$$

$$\text{The 2nd time step: } \left\| \mathbf{X}_{[N]}^{new} - \tilde{\mathbf{G}}_{N(2)}^{new}(\mathbf{G}_{[2]}^{\neq N})^\top \right\|_F \leq (1 + \tilde{\varepsilon}_2) \min_{\mathbf{G}_{N(2)}^{new}} \left\| \mathbf{X}_{[N]}^{new} - \mathbf{G}_{N(2)}^{new}(\mathbf{G}_{[2]}^{\neq N})^\top \right\|_F,$$

...

To obtain an upper bound on the error for all current time steps, let $\tilde{\varepsilon} = \min\{\tilde{\varepsilon}_1, \tilde{\varepsilon}_2, \dots\}$, then the following holds with a probability of at least $1 - \delta$:

$$\left\| \mathbf{X}_{[N]} - \tilde{\mathbf{G}}_{N(2)}(\mathbf{G}_{[2]}^{\neq N})^\top \right\|_F \leq (1 + \tilde{\varepsilon}) \min_{\mathbf{G}_{N(2)}} \left\| \mathbf{X}_{[N]} - \mathbf{G}_{N(2)}(\mathbf{G}_{[2]}^{\neq N})^\top \right\|_F,$$

for

$$\tilde{m} \geq \left(\frac{2\gamma R_N R_1}{\tilde{\varepsilon}} \right) \max \left[\frac{48}{\tilde{\varepsilon}} \ln \left(\frac{96\gamma R_N R_1}{\tilde{\varepsilon}^2 \sqrt{\delta}} \right), \frac{1}{\delta} \right].$$

For the non-temporal mode n , if

$$m'_n \geq \left(\frac{2\gamma R_n R_{n+1}}{\varepsilon'_n} \right) \max \left[\frac{48}{\varepsilon'_n} \ln \left(\frac{96\gamma R_n R_{n+1}}{\varepsilon'^2_n \sqrt{\delta}} \right), \frac{1}{\delta} \right],$$

we have

$$\left\| \mathbf{X}_{[n]} - \tilde{\mathbf{G}}_{n(2)}(\mathbf{G}_{[2]}^{\neq n})^\top \right\|_F \leq (1 + \varepsilon'_n) \min_{\mathbf{G}_{n(2)}} \left\| \mathbf{X}_{[n]} - \mathbf{G}_{n(2)}(\mathbf{G}_{[2]}^{\neq n})^\top \right\|_F.$$

Thus, setting $\varepsilon = \min\{\tilde{\varepsilon}, \varepsilon'_1, \varepsilon'_2, \dots, \varepsilon'_{N-1}\}$, the proof can be completed. \square

Along the same line, the proofs of Theorems 3.2 and 3.3 can be completed by using [18, Theorem 7] and [30, Theorem 5], respectively.

B Specific Algorithms Based on Different Sketches

Algorithm 7 Randomized streaming TR decomposition with uniform sampling (rSTR-U)

Input: Initial tensor \mathcal{X}^{init} , TR-ranks R_1, \dots, R_N , new data tensor \mathcal{X}^{new} and sampling size m

Output: TR-cores $\{\mathcal{G}_n \in \mathbb{R}^{R_n \times I_n \times R_{n+1}}\}_{n=1}^N$

// Initialization stage

- 1: Using TR-ALS-Sampled (uniform) or other algorithms to decompose \mathcal{X}^{init} into TR-cores $\mathcal{G}_1, \dots, \mathcal{G}_N$

```

2: for  $k = 1, \dots, N$  do
3:    $\text{idxs}(:, k) \leftarrow \text{RANDSAMPLE}(I_k, m)$ 
4:    $(\mathcal{G}_k)_S \leftarrow \mathcal{G}_k(:, \text{idxs}(:, k), :)$ 
5: end for
6: for  $n = 1, \dots, N - 1$  do
7:   Let  $\mathcal{G}_S^{\neq n}$  be a tensor of size  $R_{n+1} \times m \times R_{n+1}$ , where every lateral slice is an
    $R_{n+1} \times R_{n+1}$  identity matrix
8:   for  $k = n + 1, \dots, N, 1, \dots, n - 1$  do
9:      $\mathcal{G}_S^{\neq n} \leftarrow \mathcal{G}_S^{\neq n} \boxtimes_2 (\mathcal{G}_k)_S$ 
10:  end for
11:   $\mathbf{X}_{S[n]}^{\text{init}} \leftarrow \text{MODE-N-UNFOLDING}(\mathcal{X}(\text{idxs}(:, 1), \dots, \text{idxs}(:, n - 1), :, \text{idxs}(:, n + 1), \dots, \text{idxs}(:, N)))$ 
12: end for
13: for  $n = 1, \dots, N - 1$  do
14:    $\mathbf{P}_n \leftarrow \mathbf{X}_{S[n]}^{\text{init}} \mathbf{G}_{S[2]}^{\neq n}$ 
15:    $\mathbf{Q}_n \leftarrow (\mathbf{G}_{S[2]}^{\neq n})^\top \mathbf{G}_{S[2]}^{\neq n}$ 
16: end for
17: for  $\tau = 1, \dots, t$  time steps do
  // Update stage for temporal mode
18:   Let  $\mathcal{G}_S^{\neq N}$  be a tensor of size  $R_1 \times m \times R_1$ , where every lateral slice is an  $R_1 \times R_1$ 
  identity matrix
19:   for  $k = 1, \dots, N - 1$  do
20:      $\mathcal{G}_S^{\neq N} \leftarrow \mathcal{G}_S^{\neq N} \boxtimes_2 (\mathcal{G}_k)_S$ 
21:   end for
22:    $\mathbf{X}_{S[N]}^{\text{new}} \leftarrow \text{MODE-N-UNFOLDING}(\mathcal{X}^{\text{new}}(\text{idxs}(:, 1), \dots, \text{idxs}(:, N - 1), :))$ 
23:    $\mathbf{G}_{N(2)}^{\text{new}} \leftarrow \mathbf{X}_{S[N]}^{\text{new}} \left( (\mathbf{G}_{S[2]}^{\neq N})^\top \right)^\dagger$ 
24:    $\mathbf{G}_{N(2)} \leftarrow \begin{bmatrix} \mathbf{G}_{N(2)}^{\text{old}} \\ \mathbf{G}_{N(2)}^{\text{new}} \end{bmatrix}$  and reshape  $\mathbf{G}_{N(2)}$  to  $\mathcal{G}_N$ 
25:    $\text{idxs}(:, N) \leftarrow \text{RANDSAMPLE}(t^{\text{new}}, m)$   $\triangleright t^{\text{new}}$  is the temporal dimension of  $\mathcal{X}^{\text{new}}$ 
26:    $(\mathcal{G}_N^{\text{new}})_S \leftarrow \mathcal{G}_N^{\text{new}}(:, \text{idxs}(:, N), :)$ 
  // Update stage for non-temporal modes
27:   for  $n = 1, \dots, N - 1$  do
28:     Let  $(\mathcal{G}_{\text{new}}^{\neq n})_S$  be a tensor of size  $R_{n+1} \times m \times R_{n+1}$ , where every lateral slice is
    an  $R_{n+1} \times R_{n+1}$  identity matrix
29:     for  $k = n + 1, \dots, N, 1, \dots, n - 1$  do
30:        $(\mathcal{G}_{\text{new}}^{\neq n})_S \leftarrow (\mathcal{G}_{\text{new}}^{\neq n})_S \boxtimes_2 (\mathcal{G}_k)_S$   $\triangleright$  If  $k = N$ ,  $(\mathcal{G}_k)_S$  will be  $(\mathcal{G}_N^{\text{new}})_S$ 
31:     end for
32:      $\mathbf{X}_{S[n]}^{\text{new}} \leftarrow \text{MODE-N-UNFOLDING}(\mathcal{X}^{\text{new}}(\text{idxs}(:, 1), \dots, \text{idxs}(:, n - 1), :, \text{idxs}(:, n + 1), \dots, \text{idxs}(:, N)))$ 
33:      $\mathbf{P}_n \leftarrow \mathbf{P}_n + \mathbf{X}_{S[n]}^{\text{new}} (\mathcal{G}_{\text{new}}^{\neq n})_{S[2]}$ 
34:      $\mathbf{Q}_n \leftarrow \mathbf{Q}_n + (\mathcal{G}_{\text{new}}^{\neq n})_{S[2]}^\top (\mathcal{G}_{\text{new}}^{\neq n})_{S[2]}$ 
35:      $\mathbf{G}_{n(2)} \leftarrow \mathbf{P}_n \mathbf{Q}_n^\dagger$  and reshape  $\mathbf{G}_{n(2)}$  to  $\mathcal{G}_n$ 
36:      $\text{idxs}(:, n) \leftarrow \text{RANDSAMPLE}(I_n, m)$ 
37:      $(\mathcal{G}_n)_S \leftarrow \mathcal{G}_n(:, \text{idxs}(:, n), :)$ 
38:   end for
39: end for

```

Algorithm 8 Randomized streaming TR decomposition with leverage-based sampling (rSTR-L)

Input: Initial tensor $\mathcal{X}^{\text{init}}$, TR-ranks R_1, \dots, R_N , new data tensor \mathcal{X}^{new} and sampling size m

Output: TR-cores $\{\mathcal{G}_n \in \mathbb{R}^{R_n \times I_n \times R_{n+1}}\}_{n=1}^N$

```

// Initialization stage
1: Using TR-ALS-Sampled or other algorithms to decompose  $\mathcal{X}^{init}$  into TR-cores
 $\mathcal{G}_1, \dots, \mathcal{G}_N$ 
2: Compute the leverage-based probability distribution  $\mathbf{p}_k$  of  $\mathbf{G}_{k(2)}$  for  $k = 1, \dots, N$ 
3: for  $k = 1, \dots, N$  do
4:    $\text{idxs}(:, k) \leftarrow \text{RANDSAMPLE}(I_k, m, \text{true}, \mathbf{p}_k)$ 
5:    $(\mathcal{G}_k)_S \leftarrow \mathcal{G}_k(:, \text{idxs}(:, k), :)$ 
6: end for
7: for  $n = 1, \dots, N - 1$  do
8:   Let  $\mathcal{G}_S^{\neq n}$  be a tensor of size  $R_{n+1} \times m \times R_{n+1}$ , where every lateral slice is an
 $R_{n+1} \times R_{n+1}$  identity matrix
9:   for  $k = n + 1, \dots, N, 1, \dots, n - 1$  do
10:     $\mathcal{G}_S^{\neq n} \leftarrow \mathcal{G}_S^{\neq n} \boxtimes_2 (\mathcal{G}_k)_S$ 
11:   end for
12:    $\mathbf{X}_{S[n]}^{init} \leftarrow \text{MODE-N-UNFOLDING}(\mathcal{X}(\text{idxs}(:, 1), \dots, \text{idxs}(:, n - 1), :, \text{idxs}(:, n + 1), \dots, \text{idxs}(:, N)))$ 
13: end for
14: for  $n = 1, \dots, N - 1$  do
15:    $\mathbf{P}_n \leftarrow \mathbf{X}_{S[n]}^{init} \mathbf{G}_{S[2]}^{\neq n}$ 
16:    $\mathbf{Q}_n \leftarrow (\mathbf{G}_{S[2]}^{\neq n})^\top \mathbf{G}_{S[2]}^{\neq n}$ 
17: end for
18: for  $\tau = 1, \dots, t$  time steps do
// Update stage for temporal mode
19:   Let  $\mathcal{G}_S^{\neq N}$  be a tensor of size  $R_1 \times m \times R_1$ , where every lateral slice is an  $R_1 \times R_1$ 
identity matrix
20:   for  $k = 1, \dots, N - 1$  do
21:     $\mathcal{G}_S^{\neq N} \leftarrow \mathcal{G}_S^{\neq N} \boxtimes_2 (\mathcal{G}_k)_S$ 
22:   end for
23:    $\mathbf{X}_{S[N]}^{new} \leftarrow \text{MODE-N-UNFOLDING}(\mathcal{X}^{new}(\text{idxs}(:, 1), \dots, \text{idxs}(:, N - 1), :))$ 
24:    $\mathbf{G}_{N(2)}^{new} \leftarrow \mathbf{X}_{S[N]}^{new} \left( (\mathbf{G}_{S[2]}^{\neq N})^\top \right)^\dagger$ 
25:    $\mathbf{G}_{N(2)} \leftarrow \begin{bmatrix} \mathbf{G}_{N(2)}^{old} \\ \mathbf{G}_{N(2)}^{new} \end{bmatrix}$  and reshape  $\mathbf{G}_{N(2)}$  to  $\mathcal{G}_N$ 
26:   Compute  $\mathbf{p}_N$  for  $\mathbf{G}_{N(2)}^{new}$ 
27:    $\text{idxs}(:, N) \leftarrow \text{RANDSAMPLE}(t^{new}, m, \text{true}, \mathbf{p}_N) \triangleright t^{new}$  is the temporal dimension of
 $\mathcal{X}^{new}$ 
28:    $(\mathcal{G}_N)_S \leftarrow \mathcal{G}_N(:, \text{idxs}(:, N), :)$ 
// Update stage for non-temporal modes
29:   for  $n = 1, \dots, N - 1$  do
30:    Let  $(\mathcal{G}_{new}^{\neq n})_S$  be a tensor of size  $R_{n+1} \times m \times R_{n+1}$ , where every lateral slice is
an  $R_{n+1} \times R_{n+1}$  identity matrix
31:    for  $k = n + 1, \dots, N, 1, \dots, n - 1$  do
32:      $(\mathcal{G}_{new}^{\neq n})_S \leftarrow (\mathcal{G}_{new}^{\neq n})_S \boxtimes_2 (\mathcal{G}_k)_S \quad \triangleright$  If  $k = N$ ,  $(\mathcal{G}_k)_S$  will be  $(\mathcal{G}_N^{new})_S$ 
33:    end for
34:     $\mathbf{X}_{S[n]}^{new} \leftarrow \text{MODE-N-UNFOLDING}(\mathcal{X}^{new}(\text{idxs}(:, 1), \dots, \text{idxs}(:, n - 1), :, \text{idxs}(:, n + 1), \dots, \text{idxs}(:, N)))$ 
35:     $\mathbf{P}_n \leftarrow \mathbf{P}_n + \mathbf{X}_{S[n]}^{new} (\mathbf{G}_{new}^{\neq n})_{S[2]}$ 
36:     $\mathbf{Q}_n \leftarrow \mathbf{Q}_n + (\mathbf{G}_{new}^{\neq n})_{S[2]}^\top (\mathbf{G}_{new}^{\neq n})_{S[2]}$ 
37:     $\mathbf{G}_{n(2)} \leftarrow \mathbf{P}_n \mathbf{Q}_n^\dagger$  and reshape  $\mathbf{G}_{n(2)}$  to  $\mathcal{G}_n$ 
38:    Recompute  $\mathbf{p}_n$  for updated  $\mathbf{G}_{n(2)}$ 
39:     $\text{idxs}(:, n) \leftarrow \text{RANDSAMPLE}(I_n, m, \text{true}, \mathbf{p}_n)$ 

```

```

40:   ( $\mathcal{G}_n$ )S ←  $\mathcal{G}_n(:, \text{idxs}(:, n), :)$ 
41:   end for
42: end for

```

Algorithm 9 Randomized streaming TR decomposition with KSRFT (rSTR-K)

Input: Initial tensor \mathcal{X}^{init} , TR-ranks R_1, \dots, R_N , new data tensor \mathcal{X}^{new} and sketch size m

Output: TR-cores $\{\mathcal{G}_n \in \mathbb{R}^{R_n \times I_n \times R_{n+1}}\}_{n=1}^N$

// Initialization stage

```

1: Using TR-KSRFT-ALS or other algorithms to decompose  $\mathcal{X}^{init}$  into TR-cores  $\mathcal{G}_1, \dots, \mathcal{G}_N$ 
2: Define random sign-flip operators  $\mathbf{D}_j$  and FFT matrices  $\mathbf{F}_j$ , for  $j \in [N]$ 
3: Mix TR-cores:  $\hat{\mathcal{G}}_n \leftarrow \mathcal{G}_n \times_2 (\mathbf{F}_n \mathbf{D}_n)$ , for  $n = 1, 2, \dots, N$ 
4: Mix initial tensor:  $\hat{\mathcal{X}}^{init} \leftarrow \mathcal{X} \times_1 (\mathbf{F}_1 \mathbf{D}_1) \times_2 (\mathbf{F}_2 \mathbf{D}_2) \cdots \times_N (\mathbf{F}_N \mathbf{D}_N)$ 
5: for  $k = 1, \dots, N$  do
6:    $\text{idxs}(:, k) \leftarrow \text{RANDSAMPLE}(I_k, m)$ 
7:   ( $\hat{\mathcal{G}}_k$ )S ←  $\hat{\mathcal{G}}_k(:, \text{idxs}(:, k), :)$ 
8: end for
9: for  $n = 1, \dots, N - 1$  do
10:  Let  $\hat{\mathcal{G}}_S^{\neq n}$  be a tensor of size  $R_{n+1} \times m \times R_{n+1}$ , where every lateral slice is an  $R_{n+1} \times R_{n+1}$  identity matrix
11:  for  $k = n + 1, \dots, N, 1, \dots, n - 1$  do
12:     $\hat{\mathcal{G}}_S^{\neq n} \leftarrow \hat{\mathcal{G}}_S^{\neq n} \boxtimes_2 (\hat{\mathcal{G}}_k)_S$ 
13:  end for
14:   $\hat{\mathcal{X}}_{S[n]}^{init} \leftarrow \text{MODE-N-UNFOLDING}(\hat{\mathcal{X}}(\text{idxs}(:, 1), \dots, \text{idxs}(:, n - 1), :, \text{idxs}(:, n + 1), \dots, \text{idxs}(:, N)))$ 
15:   $\hat{\mathcal{X}}_{S[n]}^{init} \leftarrow \mathbf{D}_n \mathbf{F}_n^* \hat{\mathcal{X}}_{S[n]}^{init}$ 
16: end for
17: for  $n = 1, \dots, N - 1$  do
18:   $\mathbf{P}_n \leftarrow \hat{\mathcal{X}}_{S[n]}^{init} \hat{\mathcal{G}}_{S[2]}^{\neq n}$ 
19:   $\mathbf{Q}_n \leftarrow (\hat{\mathcal{G}}_{S[2]}^{\neq n})^\top \hat{\mathcal{G}}_{S[2]}^{\neq n}$ 
20: end for
21: for  $\tau = 1, \dots, t$  time steps do
22:  Redefine random sign-flip operators  $\mathbf{D}_j$  and FFT matrices  $\mathbf{F}_j$ , for  $j \in [N]$ 
23:  Mix new tensor:  $\hat{\mathcal{X}}^{new} \leftarrow \mathcal{X} \times_1 (\mathbf{F}_1 \mathbf{D}_1) \times_2 (\mathbf{F}_2 \mathbf{D}_2) \cdots \times_N (\mathbf{F}_N \mathbf{D}_N)$ 
24:  Mix TR-cores:  $\hat{\mathcal{G}}_n \leftarrow \mathcal{G}_n \times_2 (\mathbf{F}_n \mathbf{D}_n)$ , for  $n = 1, 2, \dots, N - 1$ 
  // Update stage for temporal mode
25:  Let  $\hat{\mathcal{G}}_S^{\neq N}$  be a tensor of size  $R_1 \times m \times R_1$ , where every lateral slice is an  $R_1 \times R_1$  identity matrix
26:  for  $k = 1, \dots, N - 1$  do
27:     $\hat{\mathcal{G}}_S^{\neq N} \leftarrow \hat{\mathcal{G}}_S^{\neq N} \boxtimes_2 (\hat{\mathcal{G}}_k)_S$ 
28:  end for
29:   $\hat{\mathcal{X}}_{S[N]}^{new} \leftarrow \text{MODE-N-UNFOLDING}(\hat{\mathcal{X}}^{new}(\text{idxs}(:, 1), \dots, \text{idxs}(:, N - 1), :))$ 
30:   $\hat{\mathcal{X}}_{S[N]}^{init} \leftarrow \mathbf{D}_N \mathbf{F}_N^* \hat{\mathcal{X}}_{S[N]}^{init}$ 
31:   $\mathbf{G}_{N(2)}^{new} \leftarrow \Re(\hat{\mathcal{X}}_{S[N]}^{new}) \left( \Re((\hat{\mathcal{G}}_{S[2]}^{\neq N})^\top) \right)^\dagger$ 
32:   $\mathbf{G}_{N(2)} \leftarrow \begin{bmatrix} \mathbf{G}_{N(2)}^{old} \\ \mathbf{G}_{N(2)}^{new} \end{bmatrix}$  and reshape  $\mathbf{G}_{N(2)}$  to  $\mathcal{G}_N$ 
33:   $\hat{\mathcal{G}}_N^{new} \leftarrow \mathcal{G}_N^{new} \times_2 (\mathbf{F}_N \mathbf{D}_N)$ 
34:   $\text{idxs}(:, N) \leftarrow \text{RANDSAMPLE}(t^{new}, m)$   $\triangleright t^{new}$  is the temporal dimension of  $\mathcal{X}^{new}$ 
35:  ( $\hat{\mathcal{G}}_N^{new}$ )S ←  $\hat{\mathcal{G}}_N^{new}(:, \text{idxs}(:, N), :)$ 
  // Update stage for non-temporal modes

```

```

36:   for  $n = 1, \dots, N - 1$  do
37:     Let  $(\hat{\mathbf{G}}_{new}^{\neq n})_S$  be a tensor of size  $R_{n+1} \times m \times R_{n+1}$ , where every lateral slice is
an  $R_{n+1} \times R_{n+1}$  identity matrix
38:     for  $k = n + 1, \dots, N, 1, \dots, n - 1$  do
39:        $(\hat{\mathbf{G}}_{new}^{\neq n})_S \leftarrow (\hat{\mathbf{G}}_{new}^{\neq n})_S \boxtimes_2 (\hat{\mathbf{G}}_k)_S$  ▷ If  $k = N$ ,  $(\hat{\mathbf{G}}_k)_S$  will be  $(\hat{\mathbf{G}}_N^{new})_S$ 
40:     end for
41:      $\hat{\mathbf{X}}_{S[n]}^{new} \leftarrow \text{MODE-N-UNFOLDING}(\hat{\mathbf{X}}^{new}(\text{idxs}(:, 1), \dots, \text{idxs}(:, n - 1), :, \text{idxs}(:, n + 1), \dots, \text{idxs}(:, N)))$ 
42:      $\hat{\mathbf{X}}_{S[n]}^{init} \leftarrow \mathbf{D}_n \mathbf{F}_n^* \hat{\mathbf{X}}_{S[n]}$ 
43:      $\mathbf{P}_n \leftarrow \mathbf{P}_n + \mathbf{X}_{S[n]}^{new} \overline{(\mathbf{G}_{new}^{\neq n})_{S[2]}}$ 
44:      $\mathbf{Q}_n \leftarrow \mathbf{Q}_n + (\mathbf{G}_{new}^{\neq n})_{S[2]}^\top \overline{(\mathbf{G}_{new}^{\neq n})_{S[2]}}$ 
45:      $\mathbf{G}_{n(2)} \leftarrow \Re(\mathbf{P}_n) \Re(\mathbf{Q}_n)^\dagger$  and reshape  $\mathbf{G}_{n(2)}$  to  $\mathcal{G}_n$ 
46:      $\hat{\mathcal{G}}_n \leftarrow \mathcal{G}_n \times_2 (\mathbf{F}_n \mathbf{D}_n)$ 
47:      $\text{idxs}(:, n) \leftarrow \text{RANDSAMPLE}(I_n, m)$ 
48:      $(\hat{\mathcal{G}}_n)_S \leftarrow \hat{\mathcal{G}}_n(:, \text{idxs}(:, n), :)$ 
49:   end for
50: end for

```

